



Minerva Access is the Institutional Repository of The University of Melbourne

Author/s:

Eissa, O;Filkov, A;Ghodrat, M

Title:

Review of thermal behaviour of firebrands and their role in fuel bed and structure ignition

Date:

2025-05-26

Citation:

Eissa, O., Filkov, A. I. & Ghodrat, M. (2025). Review of thermal behaviour of firebrands and their role in fuel bed and structure ignition. *International Journal of Wildland Fire*, 34 (6), <https://doi.org/10.1071/WF25021>.

Persistent Link:

<https://hdl.handle.net/11343/363497>

License:

[CC-BY-NC-ND](#)

Review of thermal behaviour of firebrands and their role in fuel bed and structure ignition

Osman Eissa^{A,*}, Alexander I. Filkov^B  and Maryam Ghodrat^{A,*} 

For full list of author affiliations and declarations see end of paper

*Correspondence to:

Osman Eissa

School of Engineering and Technology,
University of New South Wales (UNSW),
Canberra, ACT 2600, Australia

Email: o.eissa@unsw.edu.au

Maryam Ghodrat

School of Engineering and Technology,
University of New South Wales (UNSW),
Canberra, ACT 2600, Australia

Email: m.ghodrat@unsw.edu.au

Received: 31 January 2025

Accepted: 23 April 2025

Published: 26 May 2025

Cite this: Eissa O *et al.* (2025) Review of thermal behaviour of firebrands and their role in fuel bed and structure ignition. *International Journal of Wildland Fire* **34**, WF25021. doi:[10.1071/WF25021](https://doi.org/10.1071/WF25021)

© 2025 The Author(s) (or their employer(s)).
Published by CSIRO Publishing on behalf of
IAWF.

This is an open access article distributed
under the Creative Commons Attribution-
NonCommercial-NoDerivatives 4.0
International License ([CC BY-NC-ND](https://creativecommons.org/licenses/by-nc-nd/4.0/))

OPEN ACCESS

ABSTRACT

Firebrands or embers are a crucial phenomenon in wildfire behaviour. Firebrands – small, burning or smouldering pieces of wood or other flammable materials – can be carried by wind considerable distances, leading to ignition of new fires ahead of the main fire front. This process, called spotting, significantly contributes to the rapid spread of fires, particularly in wildland–urban interface (WUI) areas. Spot fires pose a severe threat to people and properties. Better understanding the thermal behaviour of firebrands and their ability to ignite various natural fuel beds and structural materials is crucial for developing effective fire prevention and mitigation strategies. This paper presents a comprehensive review of recent studies investigating the thermal behaviour of firebrands and their interaction with natural and structural fuels. These intensive research efforts have focused on predicting firebrand behaviour in spot fires through experimental studies, numerical simulations and statistical modelling to identify factors influencing ignition likelihood. This review explores the mechanisms through which firebrands interact with vegetative and building materials, focusing on ignition and subsequent fire spread. Critical factors, such as material composition, moisture content and firebrand accumulation, are discussed. This study also identifies critical knowledge gaps and proposes future research directions to ultimately contribute to more effective wildfire mitigation and management strategies.

Keywords: embers, firebrand pile, firebrand shower, firebrands, ignition, spot fire, thermal behaviour, wildfires, WUI.

Introduction

Over the past few decades, there has been a notable increase of wildfires globally (Manzello *et al.* 2013; Donovan *et al.* 2023). They have caused a wide range of significant impacts, including the release of carbon dioxide, loss of biodiversity, destruction of structures and contribution to global warming (Manzello *et al.* 2013; Thomas *et al.* 2017). Wildfires can rapidly move from wildlands to residential zones, leading to wildland–urban interface (WUI) fires and posing substantial risks to both human populations and property globally (Fernandez-Pello 2017; Kramer *et al.* 2018; Radeloff *et al.* 2018). For instance, in 2014, Chile experienced severe wildfires that, in just 5 days, resulted in the deaths of 15 people, injured over 500, destroyed more than 2900 homes, burned 10 km² and prompted the evacuation of ~12,500 individuals (Reszka and Fuentes 2014). In 2017, Portugal was devastated by fires that consumed over 5000 km² and resulted in at least 112 deaths (Viegas 2018). During the US 2018 Camp Fire, over 18,000 structures were destroyed (Attorney 2020). During the 2019–2020 Australian bushfire season (Filkov *et al.* 2020; Henriques-Gomes 2020; Tiernan and O'Mallon 2020; Ulpiani *et al.* 2020), nearly 5900 buildings were destroyed, and the lives of at least 34 people were lost. Significant WUI fires have also occurred in other parts of the world (Lampin-Maillet *et al.* 2010; Claridge and Spearpoint 2013). WUI fires have become an increasing threat as more people move into fire-prone regions and urbanisation continues to spread (Haynes *et al.* 2020; Filkov *et al.* 2023).

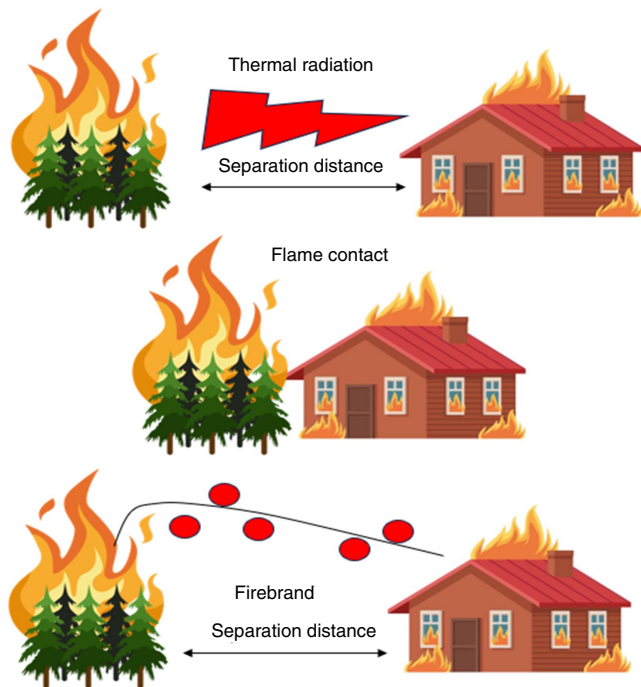


Fig. 1. Fire spread mechanisms in the WUI: thermal radiation, direct flame contact and firebrands.

Fires spread to the WUI through three fundamental pathways: radiant exposure, direct flame contact exposure and firebrands, as shown in Fig. 1 (Caton *et al.* 2017; Gaudet *et al.* 2020; Filkov *et al.* 2023). Among these pathways, firebrands, also known as embers or burning debris, have been recognised as one of the primary causes of ignition and rapid fire spread in the WUI (Manzello *et al.* 2005a; Ganteaume *et al.* 2011). Firebrands can be lifted by the fire's plume, carried by wind over a considerable distance and then ignite target fuel on contact. This phenomenon is known as ember or firebrand spotting (Albini 1979; Koo *et al.* 2010), shown in Fig. 2. For instance, post-fire investigations indicate that one out of every three destroyed homes were due to direct ember ignitions (Maranghides and Mell 2011; Thomas *et al.* 2021). In the Grass Valley Fire in the USA, 199 homes were destroyed by firebrands just during the first day (Cohen and Stratton 2008). Moreover, over 50% of the destroyed houses during the Canberra bushfire (2003) (Leonard and Blanche 2005) were due to embers. Firebrands are generated as a result of the combustion and ignition of vegetation, structures and other combustible materials that serve as fuel (Manzello *et al.* 2008a; Rissel and Ridenour 2013; Zhou *et al.* 2019; Wadhvani *et al.* 2022). During intense wildfires, owing to their lightweight nature, these particles can generate ember storms, significantly accelerating fire spread by igniting spot fires far from the primary fire zone. This allows the fire to cross natural or human-made barriers, known as firebreaks (Tarifa *et al.* 1965; Albini 1983; Karimpour and Kaye 2012; Manzello 2019; Dossi and Rein 2022; Dossi *et al.* 2025). For

example, these flying debris were able to initiate new spot fires up to 33 km from the main fire during the Victorian bushfires in 2009 (Cruz *et al.* 2012).

One of the critical aspects of spotting is the ignition of structural materials or vegetation by firebrands (Moghtaderi *et al.* 2007; Manzello 2019). This ignition will occur if the firebrand possesses enough energy to heat, dry and ignite the fuel. The ignition process is significantly affected by various factors, such as firebrand properties involving firebrand thermal behaviour, conditions (smouldering or flaming) and accumulation patterns (Almeida *et al.* 2011; Santamaria *et al.* 2015; Hakes *et al.* 2019; Suzuki and Manzello 2020b; Lin *et al.* 2024b). Furthermore, the shape, mass and size, along with the remaining heat after travel and the contact area between these firebrands and fuel bed (Filkov *et al.* 2017; Warey 2018; Salehizadeh *et al.* 2021), environmental conditions (Kasymov *et al.* 2016; Song *et al.* 2017; Yan *et al.* 2024), fuel arrangement and moisture content (Cawson *et al.* 2022) significantly influence ignition probability and fire spread.

Understanding the thermal behaviour of these firebrands, including their temperature and heat flux, as well as the thermal interaction between firebrands and the receptive fuel, will enable us to predict the potential of these particles to ignite new spot fires. Moreover, it is crucial for predicting fire spread in WUI communities and developing fire management strategies through utilisation of fire-resistant materials and implementing landscaping practices.

This paper provides a comprehensive review of the thermal behaviour of firebrands focusing on the measurement of their temperature and heat flux and examining their critical role in the ignition process. Additionally, the paper explores the characteristics of firebrands, such as size, shape, mass, number and accumulation patterns. To achieve this, we focused on the main factors that affect firebrands causing spot fires. This focus guided the structure of the article as follows:

First section: thermal behaviour of firebrands:

- Thermal behaviour of an individual firebrand
- Thermal behaviour of accumulated firebrands.

Second section: ignition of vegetative fuel bed by firebrands:

- Ignition by individual natural firebrands
- Ignition by metal firebrands
- Ignition by accumulated firebrands
- Ignition by firebrand showers.

Third section: ignition of structures by firebrands:

- Influence of firebrand characteristics
- Influence of structure characteristics
- Ignition of structure by firebrand showers
- Enhancing the resilience of buildings against firebrand attacks.

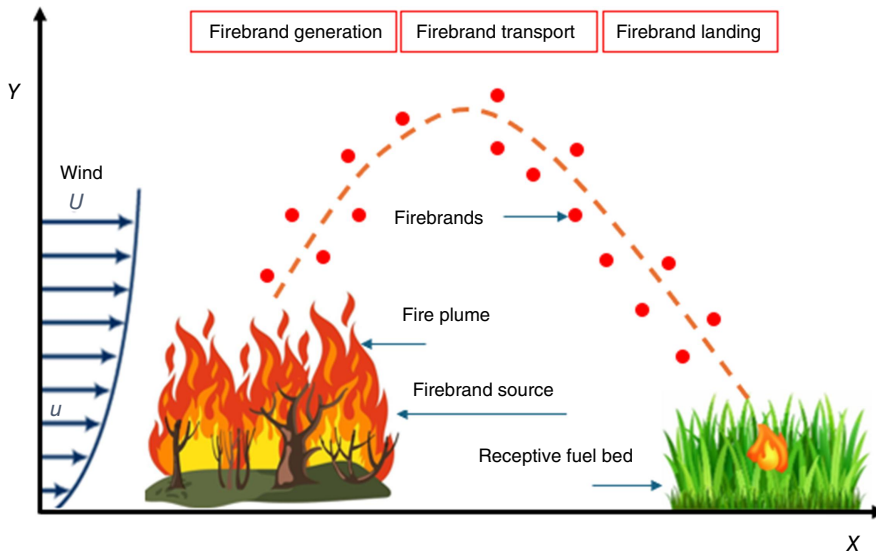


Fig. 2. The three processes of spot fire phenomena caused by firebrands.

Thermal behaviour of firebrands

The thermal behaviour of firebrands, such as temperature and heat flux, plays a crucial role in influencing the ignition of a fuel bed (Wessies and Yang 2023). These parameters of firebrands are significantly influenced by several factors. Wind serves as the primary source of oxygen delivery for the combustion zone, thereby increasing the firebrand's temperature and the heat flux (Kim and Sunderland 2019; Mensch *et al.* 2023a). The orientation of the firebrand in relation to the wind after landing is also crucial, as a perpendicular orientation generally results in more stable and intense combustion compared with a parallel one (Abul-Huda and Bouvet 2021). In addition, the material properties and chemical composition of the firebrand play a significant role in the oxidation rate and overall heat release. These factors, in turn, influence the formation of ash on the firebrand's surface, which can insulate the underlying firebrands, thereby affecting both temperature and heat flux (Wong *et al.* 2022).

In this section, we examine the effect of these factors on the thermal behaviour of firebrands by reviewing data on their temperature and heat flux, focusing on both individual and accumulated firebrands. The studies that measured the thermal behaviour of deposited firebrands are summarised in Tables 1 and 2.

Thermal behaviour of an individual firebrand

Temperature measurement

The temperature at which a firebrand's surface glows is a critical factor in two key aspects, its burning rate and its ability to ignite a target fuel on landing (Urban *et al.* 2019b). However, factors such as variations in material, shape, size, moisture content and environmental conditions, like wind speed, can significantly influence firebrand temperature, heat release

and overall energy output during flight and transport (Green and Kaye 2019; Ju *et al.* 2024). For instance, cylindrical firebrands show a more even distribution of temperature compared with irregular shapes (Hedayati *et al.* 2019; Abul-Huda and Bouvet 2021; Tao *et al.* 2021). Furthermore, the type of fuel from which firebrands are generated, such as vegetation or timber material, has a significant impact on the thermal characteristics of firebrands owing to the varying combustion and chemical characteristics (Ellis 2000; Manzello *et al.* 2007a; Prohanov *et al.* 2020). A range of measurement methods, including the use of thermocouples to measure the surface temperature of a firebrand, provides real-time temperature data as the firebrand burns (Manzello *et al.* 2009b). Infrared thermography, which enables the indirect measurement of temperature, has been used to capture both spatial and temporal temperature distributions across the firebrand surface, offering valuable insights into heating patterns (Urban *et al.* 2019b; Baldwin and Sunderland 2023). However, the accuracy of the infrared camera (IR) technique is affected by variations in emissivity, particularly owing to the formation of ash layers. Studies have shown that the formation of an insulating ash layer reduces the firebrand surface temperature while prolonging combustion duration, as examined by Wong *et al.* (2022). Their study used an inverse heat transfer method based on thermograms recorded by IR cameras with an emissivity of 0.9, and a 2D numerical model, revealing that vegetative firebrands present lower temperatures, as shown in Fig. 3, but longer burning times compared with structural firebrands owing to the formation of an ash layer on the outer surface of the firebrands, which acts as an insulation, and slows the oxidation process of the char core.

Additional experimental exploration using IR cameras with an emissivity of 0.6 was conducted by Manzello *et al.* (2009b), who measured the surface temperature of a glowing firebrand under airflow. They found that the average surface temperature of a cylindrical glowing firebrand made

Table 1. Summary of studies on thermal behaviour of individual firebrands.

Ref.	Measured parameters	Experimental conditions	Findings
Manzello <i>et al.</i> (2009b)	Surface temperature and heat flux of cylindrical glowing firebrand	<ul style="list-style-type: none"> IR imaging of the surface temperature of a firebrand Wind speed: 1.3 and 2.4 m/s 	<ul style="list-style-type: none"> The maximum measured temperature and heat flux were 700°C and 34.2 kW/m² respectively at an airflow of 2.4 m/s
Kim and Sunderland (2019)	Surface temperature of cylindrical firebrands	<ul style="list-style-type: none"> Diameter: 6.4 mm, length: 2 cm Colour pyrometry technique combining ratio pyrometry, based on green/red pixel ratios, and greyscale pyrometry was utilised 	<ul style="list-style-type: none"> The measured temperatures ranged from 750 to 1070°C with a mean of 930°C Thermocouple measurements showed 230°C lower compared with colour pyrometry
Urban <i>et al.</i> (2019b)	Mapping of firebrand surface temperature	<ul style="list-style-type: none"> Firebrand diameter: 6.5, 9.5, 11, 15.9 mm Wind speed: 1.0–4.0 m/s 	<ul style="list-style-type: none"> Glowing temperatures ranged 750–950°C Airflow velocity and ash accumulation significantly influence the surface temperature of firebrands
Bearinger <i>et al.</i> (2021b)	Temperature and heat flux of firebrands	<ul style="list-style-type: none"> Firebrand configuration: cylindrical, cuboid Wind speed: 0.5–2 m/s 	<ul style="list-style-type: none"> The cuboid firebrand exhibited a higher peak temperature than cylindrical firebrand When the wind speed increased from 1 to 2 m/s, the heat flux value nearly doubled
Wong <i>et al.</i> (2022)	Temperature and heat flux of vegetation and structure firebrands	<ul style="list-style-type: none"> Firebrand type: vegetation firebrand (oak branch), structure firebrand (oak dowels) Wind speed: 1.0, 2, 3.5 m/s 	<ul style="list-style-type: none"> Structure firebrands have a higher surface temperature and heat flux compared with vegetation firebrands owing to the formation of an ash layer that enhances thermal resistance and decreases oxygen transport
Mensch <i>et al.</i> (2023a)	Heat flux and heating duration of disc-shaped firebrands	<ul style="list-style-type: none"> Firebrand material: birch wood discs (31.75 mm diameter, 10.6 mm thickness) Wind speed: 0.05–1.6 m/s 	<ul style="list-style-type: none"> The disc-shaped birch firebrand exhibited an average peak heat flux of 45 kW/m² An increase in total heat transfer, heating duration and mass consumption with higher flow velocity

from ponderosa pine, with a diameter of 10 mm and a length of 76 mm, ranged from 500–600 to 650–700°C for airflows of 1.3 and 2.4 m/s, respectively, as shown in Fig. 4. In contrast, Fateev *et al.* (2017) reported higher average surface temperatures, ranging from 700 to 900°C, under airflow conditions of 1–3 m/s and a temperature of 80°C for a pine bark firebrand with linear dimensions of 15, 20, 30 mm and a thickness of 4–5 mm. These notable variations in firebrand temperature highlight the influence of firebrand material and shape on the formation of an ash layer, which insulates the char core and slows the oxidation process, as well as the impact of airflow speed and temperature on the surface temperature of firebrands.

Other researchers have employed the colour pyrometry technique to measure the surface temperature of firebrands. In contrast to IR methods, colour pyrometry does not require accurate knowledge of the material's emissivity, which is often affected by the accumulation of ash on the firebrand's surface (Urbas *et al.* 2004; Kim and Sunderland 2019). This technique analyses the ratios of red, green and blue colour intensities to accurately determine the surface temperature with high spatial resolution, all without disrupting the firebrand combustion process (Urbas *et al.* 2004; Lu *et al.* 2008). For example, in Kim and Sunderland (2019) and Baldwin and Sunderland (2023), an imaging ember pyrometer was developed to measure the temperature of a cylindrical firebrand with a diameter of 6.4 mm and a length of 2 cm. A hybrid approach combining ratio pyrometry, based on green/red pixel ratios, and greyscale

pyrometry was used to estimate the surface temperature of firebrands. This method achieved a high spatial resolution of 17 µm, a signal-to-noise ratio of 530 and an estimated uncertainty of ± 20°C. The measured temperatures ranged from 750 to 1070°C, with a mean of 930°C. Interestingly, when compared with the pyrometer, fine bare-wire thermocouples underpredict the firebrand mean temperature by 230°C owing to quenching effects and imperfect thermal contact.

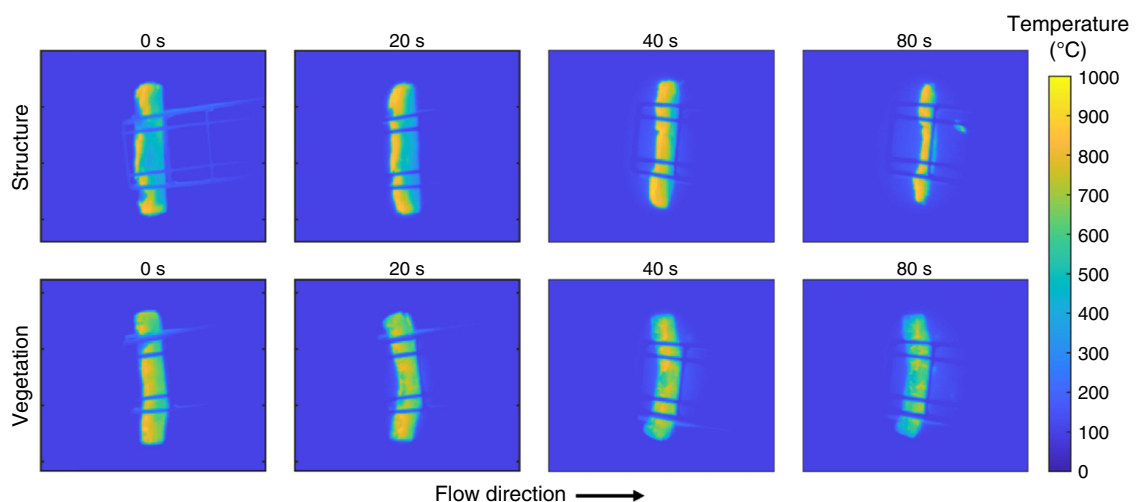
This range of temperature measurements also align with the findings of Urban *et al.* (2019b) who employed colour pyrometry to assess the surface temperature of glowing firebrands under varying airflow conditions ranging from 1 to 4 m/s. The results indicate that firebrand temperature increases with increasing airflow, with temperatures ranging from 750°C at 1 m/s to 950°C at 4 m/s, and maximum temperatures reaching up to 1100°C. Furthermore, the study highlighted temperature variations caused by periodic removal of ash by the passing air. This ash reduces the effectiveness of measuring methods, such as IR cameras, owing to its lower emissivity compared with charring wood, as also observed by Wong *et al.* (2022). However, this challenge can be overcome by using colour pyrometry to accurately measure firebrand temperatures.

Heat flux measurements

Quantifying the heat flux emitted by firebrands is crucial for evaluating their potential to ignite surrounding fuel beds or building materials. Researchers often employ heat flux

Table 2. Summary of studies on thermal behaviour of accumulated firebrands.

Ref.	Measured parameters	Experimental conditions	Findings
Thomas <i>et al.</i> (2018)	Net heat flux from glowing firebrands into substrate	<ul style="list-style-type: none"> Firebrand mass: 50, 100 and 200 g Firebrand temperature: 400 and 800°C Deposition area: $d = 50, 100$ mm 	<ul style="list-style-type: none"> Sustained smouldering accumulations, peak heat flux and burning duration are significantly influenced by accumulation mass, deposition area and initial temperature Peak heat flux measurements varied between 30 and 80 kW/m² (gauge) and 4–9 kW/m² (net)
Hakes <i>et al.</i> (2019)	Thermal energy and heat release from glowing firebrands	<ul style="list-style-type: none"> Initial diameter: 6.35, 9.52 and 12.7 mm Firebrand mass: 0.1–9.6 g 	<ul style="list-style-type: none"> Smaller diameters and larger mass of firebrands showed higher height flux and net heat release Under windy conditions, increased oxygen transport resulted in an increase in the heat flux value
Salehizadeh <i>et al.</i> (2021)	Temperature and smouldering time of firebrand	<ul style="list-style-type: none"> Firebrand mass: 4, 8 and 16 g Wind speed: 0.5–2 m/s 	<ul style="list-style-type: none"> The average temperature ranged from 500 to 700°C for the 16 g pile, and 400°C for the 4 g pile An increase in particle size results in longer smouldering time
Tao <i>et al.</i> (2021)	Heat flux	<ul style="list-style-type: none"> Firebrand type: pine bark and eucalyptus sticks, birch dowels Wind speed: 0.5–1.4 m/s Firebrand mass: 4 g 	<ul style="list-style-type: none"> At higher wind speeds, the natural fuel firebrands yielded higher heat flux compared with artificial fuels
Lattimer <i>et al.</i> (2022)	Temperature of firebrand and heat flux to a surface	<ul style="list-style-type: none"> Experiments and an analytical model prediction performed on firebrands with different sizes and wind speeds for three firebrands held in a wire mesh, and a firebrand pile 	<ul style="list-style-type: none"> Decreasing the firebrand diameter leads to an increase in the surface temperature The highest heat flux was observed at the upstream leading edge of the pile compared with downstream owing to decreased air velocity The oxygen mass fraction plays a crucial role in determining the burning rate and temperature of the firebrand Higher pile porosity results in an increase in firebrand temperature owing to the higher velocities within the pile
Cantor <i>et al.</i> (2023)	Contact surface temperatures of different type of firebrands	<ul style="list-style-type: none"> Firebrand mass: 200, 500 g. Firebrand type: <i>Eucalyptus</i> and pine, pine charcoal and conventional wood Wind speed: 1.3 m/s 	<ul style="list-style-type: none"> Proposed a standard firebrand accumulation temperature curve with max. 480°C A positive relationship between the presence of wind and duration of maximum temperature
De Beer <i>et al.</i> (2023b)	Heat flux of firebrand pile	<ul style="list-style-type: none"> Pile covering density: 0.06 and 0.16 g/cm² Wind speed: 0.9–2.7 m/s 	<ul style="list-style-type: none"> The average heat flux from the pile was found to be in the range from 28 to 80 kW/m²

**Fig. 3.** Average temperature measurements of vegetation and structure firebrands (Wong *et al.* 2022) (with permission from Elsevier, licence no. 5804601186461).

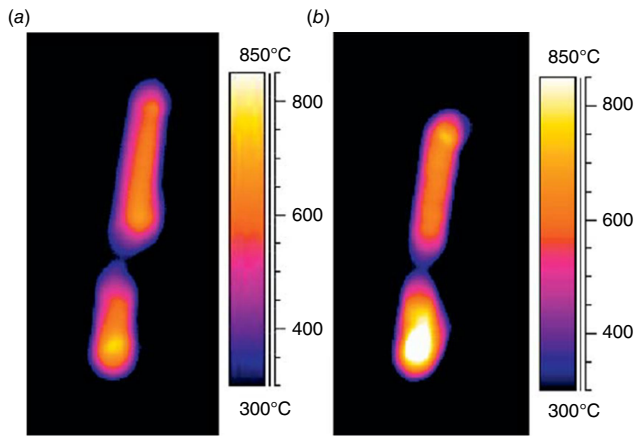


Fig. 4. IR images of the surface temperature of a glowing firebrand under the effect of airflow: (a) 1.3 m/s, and (b) 2.4 m/s (Manzello et al. 2009b) (with permission from Elsevier, licence no. 5804601510843).

sensors (Tao et al. 2021) and thin-skin calorimeters (TSCs) (Mensch et al. 2023a) to measure the radiative and convective heat fluxes. Others employ advanced techniques such as inverse heat transfer methods to evaluate the heat flux of glowing firebrands. This approach estimates heat flux by analysing the temperature increase of a surface exposed to heat, considering factors such as energy storage, conduction, and both radiative and convective heat transfers to the surface (Thomas et al. 2018). For example, Mensch et al. (2023a) proposed a novel approach for measuring the average peak net heat flux of a glowing disc firebrand using a TSC under various airflow conditions from 0.05 to 1.6 m/s. Their findings showed that the average peak net heat flux from a disc-shaped birch firebrand was 45 kW/m². Further expanding on firebrand material properties, in Mensch et al. (2023b), the effect of different firebrand wood types and wind speeds on peak heat flux, total heating and duration of heating from the firebrand was investigated. Firebrands were generated from disc-shaped samples made of four different wood types: oak, western red cedar, pine and birch. The results revealed that these parameters vary across wood types, with oak and cedar yielding lower values, whereas pine and birch showed higher heat flux and heating duration. Specifically, peak heat flux values were recorded at 60 kW/m² for pine, 74 kW/m² for birch and 62 kW/m² for cedar, whereas oak demonstrated a significantly lower peak value of 40 kW/m² under airflow conditions of 0.6 m/s. In contrast, Manzello et al. (2009b) performed a heat transfer analysis using firebrand surface temperature measurements obtained from an IR camera to estimate the heat flux from a cylindrical glowing firebrand made from ponderosa pine subjected to airflow. The results indicated that the estimated heat flux was 23.4 kW/m² for a firebrand exposed to an airflow of 1.3 m/s and this increased to 34.2 kW/m² when the airflow was raised to 2.4 m/s. These variations highlight how both firebrand shape and

material significantly affect heat flux, with disc-shaped firebrands resulting in higher peak values than cylindrical ones, even at lower wind speed, additionally indicating the effect of measurement techniques on the heat flux from the firebrands, as TSC provides a direct net heat flux measurement, whereas IR thermography relies on surface temperature estimations, which are affected by the formation of ash on the outer surface. These findings also highlight the influence of measurement techniques, as TSC provides a direct measurement that minimises heat losses and poor thermal contact, whereas IR thermography relies on surface temperature estimations, which can be affected by ash formation on the firebrand's outer surface.

Similarly, Wong et al. (2022) used an inverse heat transfer method based on the temperature rise of the firebrand's surface to estimate the average heat flux of both structural (oak dowels) and vegetative (red oak, *Quercus rubra*) firebrands and reported peak heat fluxes of 21.9 and 23.5 kW/m², respectively, at a wind speed of 1 m/s. Their findings emphasise that material composition plays a key role in heat flux, with less dense woods (structural firebrands) generating higher peak heat flux values than denser materials (vegetative firebrands), which aligns with the observations made by Mensch et al. (2023b). However, the heat flux from the vegetative firebrand decreases more gradually compared with the structural firebrand. This slower reduction in heat flux from the vegetative firebrand can be attributed to its relatively constant surface area throughout the burning process due to the formation of a layer of ash compared with the structural firebrand.

Another experimental study used an inverse heat transfer method using the surface temperature IR thermographs to quantify the heat flux from the firebrand to adjacent surfaces (Beainger et al. 2021b). Different shapes and sizes of firebrands were tested, including cylindrical and cuboid shapes with varying notches to determine how geometry affects heat transfer. The cuboid-shaped firebrands tested had identical dimensions (6.35 × 6.35 × 38.1 mm); however, each featured different notches on their faces. Additionally, a shorter cuboid, measuring 25.4 mm in length, and a cylindrical firebrand 6.35 mm in diameter and 38.1 mm long, were also tested. The wind speed varied in the range of 0.5–2.1 m/s with different orientations, parallel and perpendicular, to the firebrand. Fig. 5 illustrates the heat flux measurements of these configurations. The results indicate that the cylindrical-shaped firebrand produced lower heat flux compared with the cuboid-shaped firebrands. Notches in the firebrands tended to increase heat flux owing to enhanced radiation from the oxidising surfaces within the notches. The measured heat flux from a single firebrand ranged between 30 and 105 kW/m². It was noted that the orientation of the firebrand to the wind had a significant effect on the magnitude and duration of the heat flux.

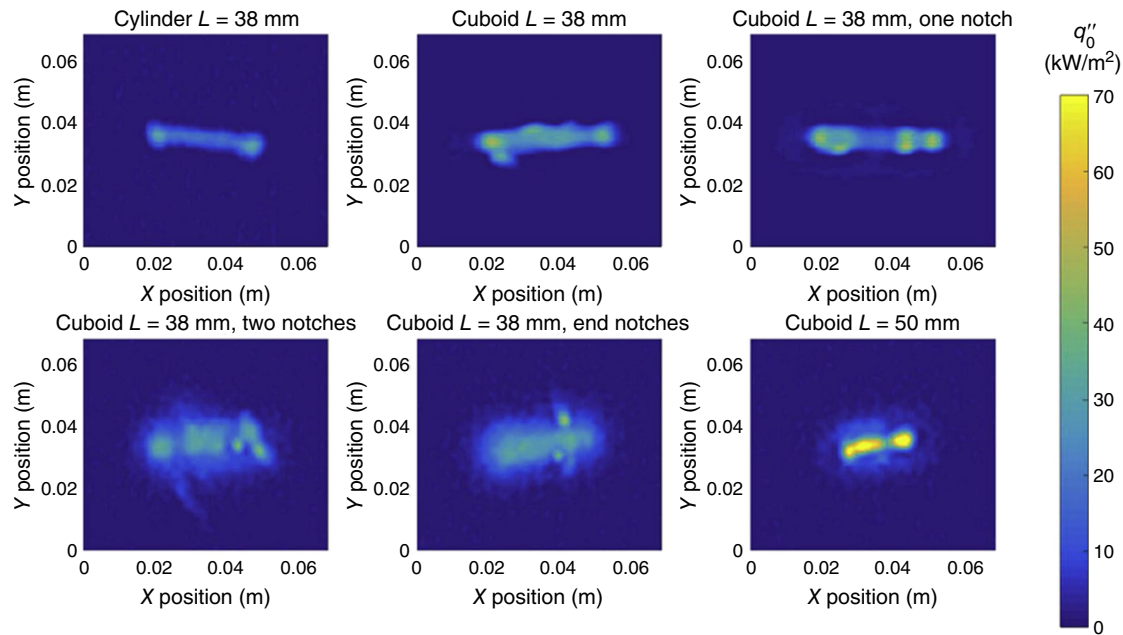


Fig. 5. The impact of firebrand shape and configuration on heat flux distributions (Bearinger *et al.* 2021b) (with permission from Elsevier, licence no. 5804610244013).

Adusumilli and Blunck (2022, 2023) investigated the effects of different wood species and moisture contents on the size and heat flux of firebrands generated from burning trees and shrubs. The study utilised fire-resistant fabric to capture char marks left by falling firebrands, which were then used to estimate heat flux. The wood species analysed included Douglas-fir, ponderosa pine and sagebrush, with moisture contents ranging from 8 to 72%. The results revealed that the char marks and heat flux of firebrands varied significantly depending on the species and moisture content. Moreover, Douglas-fir and sagebrush firebrands generally produced larger char marks and higher heat fluxes compared with ponderosa pine. This difference was attributed to variations in shape and moisture content.

Thermal behaviour of accumulated firebrands

A review of relevant studies, summarised below, highlights that the accumulation of firebrands in the form of a pile significantly impacts the thermal behaviour and burning intensity of these particles, particularly affecting the temperature and heat flux generated by firebrand piles (Bearinger *et al.* 2021a; Banagiri *et al.* 2023). When these burning particles accumulate, they form an upper layer of burning material that can insulate the underlying particles, contributing to a reduction in convective and radiative heat losses from these particles to the surroundings, and enhancing re-radiation within the pile, leading to higher overall temperatures, heat fluxes and stored energy for a longer time compared with single firebrands. This presents a higher risk of igniting adjacent fuel beds or structures (Wong *et al.*

2022). In this section, we highlight the effect of factors such as mass, porosity and wind on the thermal behaviour of firebrands by reviewing their impact on temperature and heat flux measurements. Table 2 summarises studies on the thermal behaviour of accumulated firebrands.

Temperature measurement

Understanding the temperature distribution within piles of accumulated firebrands is crucial for analysing their thermal behaviour and ignition potential. Numerous experimental studies have employed various techniques to measure temperatures in accumulated firebrands. Thin-skin calorimeters, consisting of multiple thermocouples positioned at different locations within the pile, have been widely used to obtain spatial and temporal temperature data (Thomas *et al.* 2018; Salehizadeh *et al.* 2021; Tao *et al.* 2021). This method represents an estimation of the temperature beneath the firebrand pile or between the pile and an inert board, providing representative temperatures for both the centre and the perimeter of the pile. Additionally, infrared thermography has been employed to visualise surface temperature distributions and identify hot spots within the piles (Lattimer *et al.* 2022). For example, Salehizadeh *et al.* (2021) characterised the thermal condition of three piles with masses of 4, 8 and 16 g having bulk densities of 38.3, 46.8 and 54 kg/m³ respectively using TSCs. It was found that, as illustrated in Fig. 6, both the mass of the pile and wind speed significantly impacted the firebrand temperature. It was observed that an increase in these variables led to higher surface temperatures. The highest peak temperature was found to be approximately 700°C, occurring with a

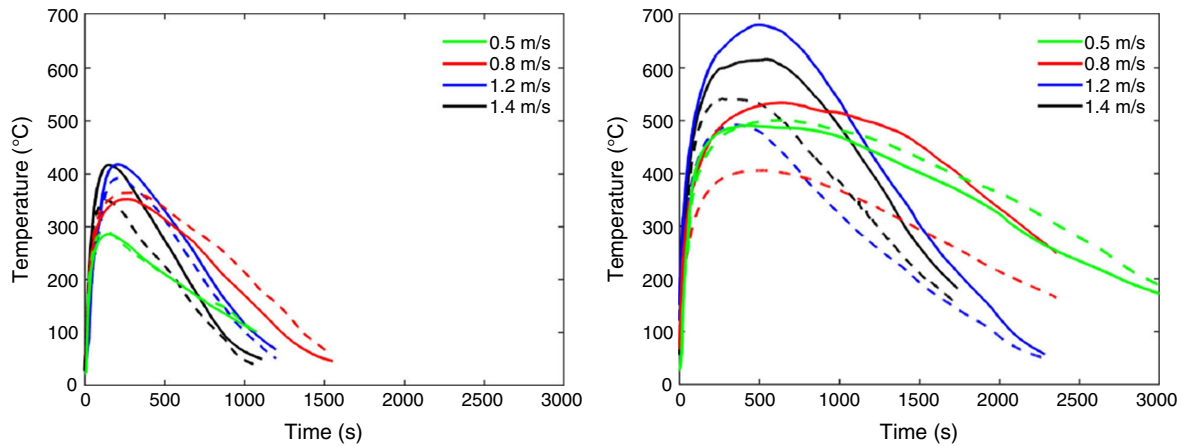


Fig. 6. Averaged temperatures for a firebrand pile using TSCs: (left) a 4 g mass pile, and (right) a 16 g mass pile. Solid lines represent inner TSCs; dashed lines represent outer TSCs (Salehizadeh et al. 2021).

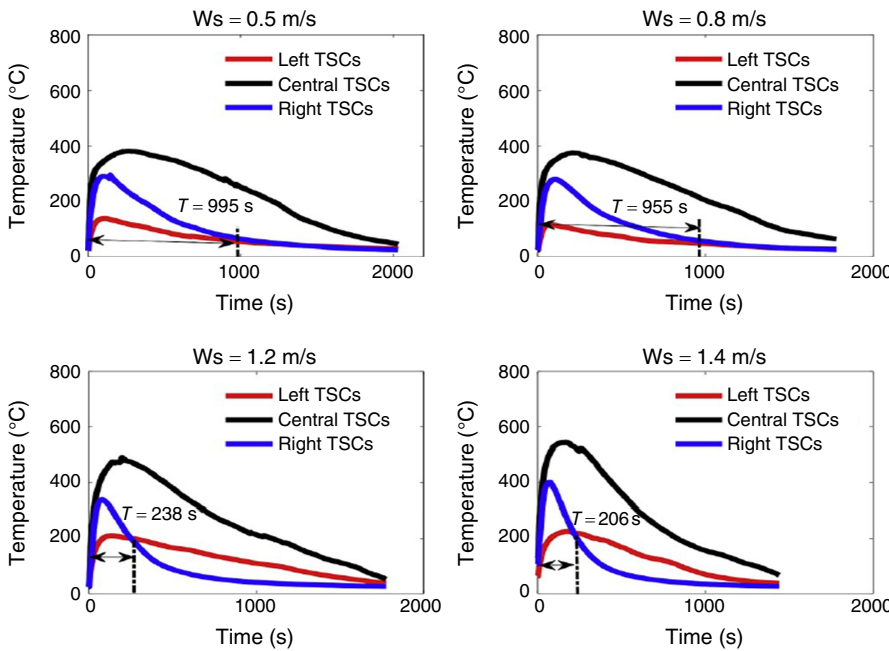


Fig. 7. The temperature distribution within a firebrand pile at three distinct areas: the upstream, centre and downstream regions of the pile (Tao et al. 2021) (with permission from Elsevier, licence no. 5819120015640). Note: W_s is wind speed.

pile mass of 16 g and a wind speed of 1.2 m/s, whereas the 4 g pile reached only $\sim 400^\circ\text{C}$, a temperature range that aligns with the findings of Tao et al. (2021) for the lowest mass pile. Furthermore, Tao et al. (2021) observed spatial temperature variations within firebrand piles focused on the distribution of temperatures in three distinct areas: the upstream, centre and downstream regions of the pile under different applied airflow. Their results, shown in Fig. 7, revealed that the highest temperatures occur in the centre region compared with other regions throughout the entire smouldering process. Moreover, in the final stages of smouldering, the downstream region yielded higher temperatures than the upstream region. This is attributed to the increased burning rates having consumed much of the fuel in the upstream area, leaving more fuel available downstream. In

contrast, studies by Bicelli et al. (2023) and Cantor et al. (2023) focused on developing a standardised firebrand accumulation temperature curve to assess the contact temperature between various firebrand types, including eucalyptus and pine, pine charcoal and conventional wood and a surface, revealing that the maximum firebrand contact surface temperatures recorded are in the range of $123\text{--}432^\circ\text{C}$ depending on the firebrand type.

However, Lattimer et al. (2022) developed an analytical model to explore the dynamics of firebrand piles, highlighting the significant influence of factors such as pile porosity, firebrand diameter and gas velocity on firebrand temperatures and heat transfer behaviour. It was found that the porosity within a firebrand pile plays a crucial role in determining the velocity within the pile, as decreasing porosity

leads to lower temperatures of firebrands. The reason is that piles with lower porosity exhibit reduced air velocities both at the leading edge of the pile and within the pile, slowing down the oxidation process. Moreover, they found that smaller firebrand diameters led to increased temperatures. This increase is due to a higher heat transfer coefficient associated with smaller diameters, which enhanced the burning rate. Additionally, decreasing the firebrand diameter resulted in reduced heat loss from the firebrand surface.

Heat flux measurement

Studies consistently indicate that the heat flux from piles of accumulated firebrands is considerably higher than from individual firebrands. This increase is largely due to the intricate interactions and heat transfer processes within the pile. In a pile, firebrands are grouped together, which can lead to a higher accumulation of heat due to reduced heat loss to the surrounding environment. Therefore, their collective heat release and enhanced radiative heat transfer among the particles lead to significantly higher heat flux values. Furthermore, the accumulation of firebrands in a pile enhances their insulation from some of the convective cooling effects caused by the surrounding wind, thereby elevating the heat flux values on the target surface. Techniques commonly used for heat flux measurement from firebrand piles include using water-cooled heat flux gauges or developing an inverse heat transfer analysis using IR thermography, which provides a means to visualise the surface of the pile, identifying critical hot spots (Hakes *et al.* 2019; De Beer *et al.* 2023b).

Hakes *et al.* (2019) conducted a comprehensive comparison of different techniques for measuring the thermal characteristics of glowing firebrand piles. They investigated heat flux under various conditions using a water-cooled heat flux gauge (WC-HFG) with diameters of 1.27 and 2.54 cm, as well as an array of TSCs. Although the WC-HFG introduces a cooling effect on the firebrand pile, their study demonstrated that it still provided a reliable representation of heat flux. In contrast,

the TSC array effectively captured spatial variations in heat flux. Interestingly, heat flux measurements obtained using the 2.54 cm WC-HFG were consistently lower than those from the 1.27 cm gauge, highlighting the greater cooling effect of the larger gauge. Additionally, WC-HFG measurements were slightly lower than those from the TSCs, further emphasising the impact of the gauge cooling effect. However, the study also highlighted significant limitations of the TSCs, particularly under windy conditions, where they demonstrated substantial inaccuracies in heat flux measurements. To further investigations, Hakes *et al.* (2019) expanded their analysis to examine the influence of firebrand diameter (ranging from 6.35 to 12.75 mm) and the deposited mass of the firebrand pile (ranging from 2.7 to 9.6 g) on heat flux. Their findings showed that the heat flux was primarily dependent on the deposited mass rather than the initial size of the firebrands. Moreover, as shown in Fig. 8, the average heat flux values ranged between 15 and 25 kW/m², while peak heat flux values generally fell within the range of 20–60 kW/m². Similarly, Salehizadeh *et al.* (2021) observed that the peak heat flux fluctuated between 15 and 40 kW/m² for a pile mass of 8 g exposed to wind speeds ranging from 0.5 to 1.4 m/s.

Thomas *et al.* (2018) developed an inverse heat transfer model to estimate the net heat flux of firebrand accumulations with masses of 50, 100 and 200 g on a substrate. The results showed that the peak heat flux, defined as the total incident heat flux for a given firebrand accumulation, ranged from 30 to 80 kW/m². Meanwhile, the peak net heat fluxes, defined as the portion of the incident heat flux that transferred into the substrate, ranged from 4 to 9 kW/m².

Another experimental study focused on quantifying the characteristics of glowing firebrand piles with different covering densities, 0.06 and 0.16 g cm⁻², under an applied wind speed varying from 0.9 to 2.7 m/s using an IR thermal imaging system was conducted in Alascio (2021) and De Beer *et al.* (2023b). An inverse model for temperature measurements in front and underneath the pile was developed to

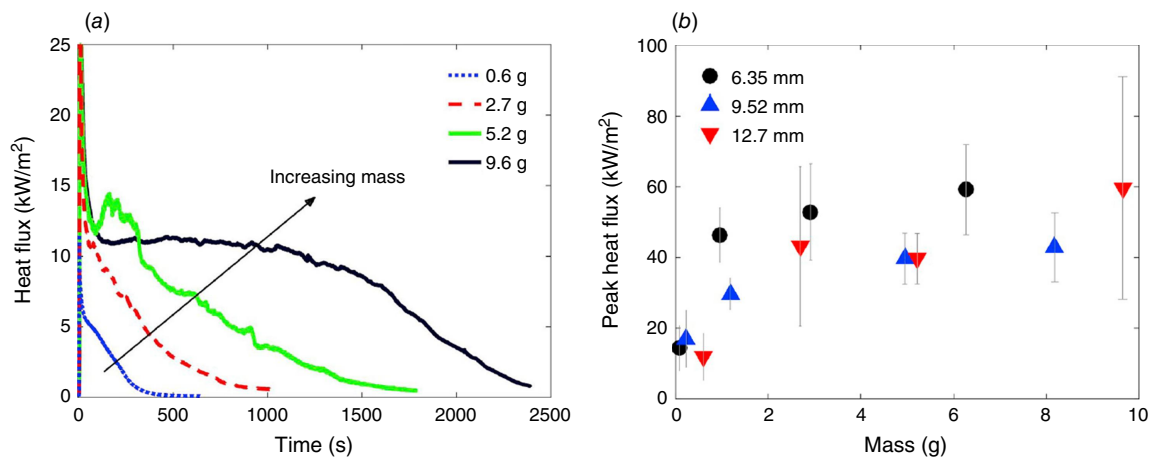


Fig. 8. The impact of the mass of the firebrand pile and firebrand diameter on the firebrand heat flux: (a) the average heat flux, and (b) the peak heat flux (Hakes *et al.* 2019) (with permission from Elsevier, licence no. 5819140027792).

predict the incident heat flux from the pile on the target fuel. Their experiments revealed that the average incident heat flux from the pile was within the range 28–80 kW/m². Meanwhile, the net heat flux ranged from 75 to 365 kW/m² in a study conducted by Cantor *et al.* (2023). They explained the higher values of the net heat flux compared with other studies was due to the use of a steel plate, which has a higher thermal conductivity, on which the firebrands were deposited.

Further investigation was conducted by Bearinger *et al.* (2021a), in which they developed a statistical model based on experimental results to study the effect of firebrand parameters such as diameter, length, wood density, type, moisture content, porosity and mass of the pile on the heat flux from a firebrand pile. They reported that artificial firebrands provided a higher heat flux compared with natural firebrands. Moreover, it was found that the wood density and moisture content did not have a significant impact on the heat flux compared with the diameter, length and mass of the pile. Additionally, increasing the porosity of the pile showed an increase in heat flux despite the shortening in burning time.

Knowledge gaps

Despite previous efforts to determine and measure thermal behaviour, temperature and heat flux aimed at assessing the susceptibility of firebrands to ignite fuel beds, there remain significant gaps in our understanding of these characteristics. One key challenge is ensuring the realism of laboratory experiments in accurately representing real-world firebrand ignition scenarios in WUI fires. Although laboratory experiments provide controlled environments for studying firebrand behaviour, they may not adequately represent the complex interactions between firebrands and natural or man-made fuels in WUI environments. In real-world scenarios, factors such as wind-driven turbulence, heterogeneous fuel bed compositions and varying atmospheric conditions introduce uncertainties that are challenging to reproduce in experimental settings. Therefore, investigating these factors is essential to gain a deeper understanding of their effect on the thermal behaviour of firebrands.

Additionally, key missing data include information on the heat transfer process, like convection and radiation losses to the surroundings and radiation exchanges between within the firebrands themselves. Another critical gap is the lack of data on the effect of how material properties, such as density, thermal conductivity, specific heat and heat of combustion, influence firebrand thermal behaviour. These properties determine the rate at which firebrands dissipate heat into their surroundings and affect their ability to maintain burning after landing on a fuel bed. Furthermore, there is limited understanding of the impact of thermal decomposition of firebrands on the remaining energy after landing on the target fuel. There is insufficient knowledge about how environmental conditions such as wind speed, temperature

and humidity influence the surface temperature and stored energy of firebrands during their flight and landing on fuel beds.

A notable gap exists regarding the impact of firebrand accumulations and their associated porosity on temperature and heat flux values within firebrand piles. The porosity of these piles, which varies with firebrand size, shape and arrangement, not only affects oxygen availability but also significantly influences the air velocity profile as it passes through the pile. This altered velocity profile impacts the oxygen supply and convection heat transfer within the pile, creating complex feedback that affects temperature distribution and sustained burning. Therefore, there is a great need to conduct research that quantifies how pile porosity, arrangement and accumulation patterns affect velocity profiles, oxygen penetration and heat transfer mechanisms. Experimental studies combined with numerical modelling of these interactions could offer valuable insights into these processes, enabling more accurate predictions of firebrand pile thermal behaviour and burning dynamics.

Ignition of vegetative fuel beds by firebrands

The ignition of recipient fuel beds by firebrands presents one of the most challenging processes in WUI fire spread. Once firebrands land on the recipient fuel bed, a series of combustion and thermal interactions between the firebrands, the fuel bed and the surrounding air starts to occur, as shown in Fig. 9, dependent on the energy of firebrands (Manzello *et al.* 2009b). When firebrands hold enough energy to dry and heat the fuel bed and initiate pyrolysis, smouldering combustion can occur, which can transition into flaming; otherwise, the firebrands cool down during this process. The burning duration and heat of combustion of firebrands significantly influence their potential to ignite spot fires (Cawson *et al.* 2022). This complex ignition process is influenced by factors such as the size, temperature, mass and condition of the firebrands (glowing or flaming) on landing (Ganteaume *et al.* 2011; Filkov *et al.* 2016). It also depends on the characteristics of the fuel bed where the firebrand lands such as the type of fuel, density, porosity and moisture content (Viegas *et al.* 2014; Álvarez *et al.* 2023; Burton *et al.* 2023; Valenzuela *et al.* 2023). Moreover, the way firebrands interact with the fuel bed on contact under different environmental conditions (temperature, humidity and wind speed) significantly affects the ignition process (Manzello *et al.* 2008a; Ellis 2015).

To ignite a fuel bed using firebrands or hot particles, a sufficient amount of heat must be transferred from the firebrand to the fuel bed to raise the temperature of the fuel to its ignition point and overcome heat losses. This process can be described by an energy balance equation where the heat generated by the firebrand must be greater than heat losses through convection and radiation as well as the heat

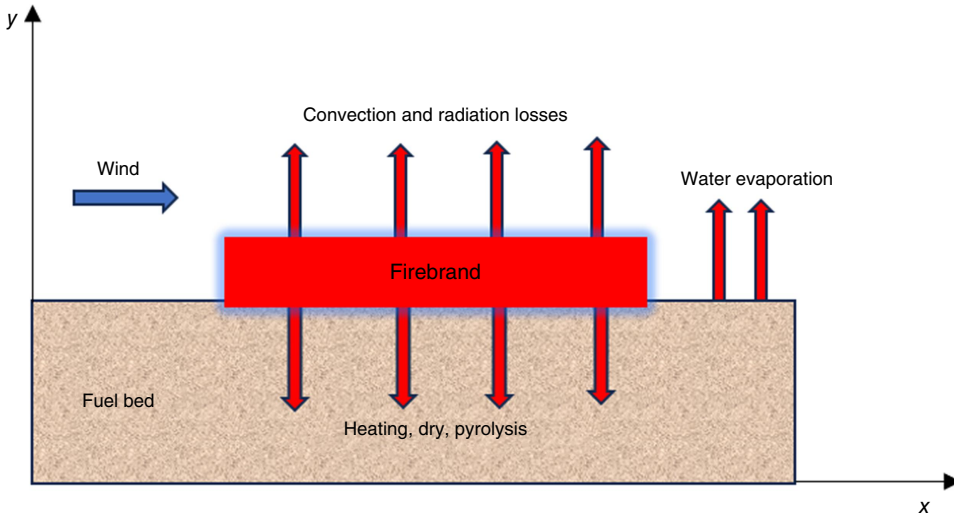


Fig. 9. Interaction between firebrand and fuel bed.

required to evaporate any moisture present in the fuel. The basic energy balance equation can be represented as follows:

$$q_{ig} \leq q_f - q_l \tag{1}$$

where q_{ig} is the minimum energy required to ignite the fuel bed, q_f is the energy released from the firebrand and q_l is the heat losses.

Assuming ignition occurs when the temperature of the fuel beds reaches the ignition temperature, q_{ig} can be expressed as follows (Suzuki and Manzello 2021b):

$$q_{ig} = \rho_{fuel} C_{fuel} V (T_{ig} - T_0) \tag{2}$$

where ρ_{fuel} is the bulk density of the fuel beds, C_{fuel} is the specific heat capacity of fuel beds, V is volume, T_{ig} is the ignition temperature and T_0 is the surrounding air temperature.

The heat generated from a glowing firebrand during the ignition process is calculated by multiplying the rate at which the firebrand loses mass during its burning time by the heat of combustion:

$$q_f = \Delta m \times HoC \tag{3}$$

where Δm is the mass loss of the firebrand, and HoC is the heat of combustion of the firebrand.

The heat losses during the ignition process occur in several ways, namely the evaporation of moisture within the fuel or reaching the ignition temperature of the dry material, as well as losses due to convection and radiation to the surrounding environment.

$$q_l = q_{evap.} + q_{conv.} + q_{rad.} \tag{4}$$

$$q_{evap.} = M [L_w + C_w (373.15 - T_0)] \tag{5}$$

$$q_{conv.} = h_{conv.} A_f (T_f - T_0) t_{ig} \tag{6}$$

$$q_{rad.} = \sigma \epsilon A_f (T_f^4 - T_0^4) t_{ig} \tag{7}$$

where $q_{evap.}$ is the heat required for water evaporation per unit mass of fuel bed, $q_{conv.}$ is the heat loss due to convection, and $q_{rad.}$ is the heat loss due to radiation (Yin *et al.* 2014). M is the moisture content, C_w is the specific heat of water (4180 J/kg K), L_w , is the heat of vaporisation (2257 kJ/kg), $h_{conv.}$ is the convection heat transfer coefficient, σ is the Stefan–Boltzmann constant, ϵ is the firebrand emissivity, A_f is the cross-sectional area of firebrand, T_f is the surface temperature of firebrand, and t_{ig} is the time to fuel bed ignition.

The heat flux from the firebrands to the fuel bed raises its temperature, initiating pyrolysis and producing volatile gases. The rate of the chemical reactions and the mass rate of pyrolysis involved in this process are governed by the Arrhenius equation, which expresses the temperature dependence of the reaction rate as:

$$k = A \exp\left(\frac{-E_a}{RT}\right) \tag{8}$$

where A is the pre-exponential factor, E_a is the activation energy, R is the gas constant, and T is temperature. Ignition occurs when heat generation from the firebrand overcomes the heat loss rate, leading to a sustained exothermic reaction in the fuel bed.

This section examines how natural fuel beds such as forest litter or vegetation can be ignited by various types of firebrands, including natural firebrands, metal firebrands, firebrand piles and firebrand showers. It explores factors that influence this ignition process, such as the firebrands' material and size, environmental conditions and the physical properties of the fuel bed. Additionally, the accumulation of multiple firebrands in the form of piles and firebrand showers is considered. Studies exploring the role of firebrands on the ignition of natural fuel beds are summarised in Table 3.

Table 3. Summary of studies on ignition of natural fuel beds by firebrands.

Ref.	Study conditions	Study parameters	Findings
Manzello et al. (2008a)	Interaction of glowing and flaming firebrand with three distinct fuel beds composed of pine needles, shredded paper and shredded hardwood mulch	<ul style="list-style-type: none"> Different sizes of cylindrical firebrands, one with 10 mm diameter and 76 mm length, and another with 5 mm diameter and 51 mm length Wind speed: 0.5 and 1.0 m/s 	<ul style="list-style-type: none"> Flame ignition was only observed with flaming firebrands Smouldering ignition of the fuel beds required a higher number of glowing firebrands
Ganteaume et al. (2009)	The likelihood of ignition of a larch fuel bed with different moisture contents and bulk densities	<ul style="list-style-type: none"> Fuel bed sample 220 × 160 × 45 mm Type of firebrands: <i>Pinus halepensis</i> twigs, bark and cone scales, <i>Quercus ilex</i> leaves, <i>Quercus suber</i> bark Air speed: 0, 0.8, 2.5 and 4.5 m/s, 3.59% < FMC < 21.2%, and 1.34 < bulk density < 46.5 	<ul style="list-style-type: none"> The time to ignition increased with increase in fuel bed moisture content, and bulk density <i>Pinus halepensis</i> cones were the firebrand type with the highest capability of ignition for all the tested conditions
Hadden et al. (2011)	Combined experimental and theoretical study involving the use of spherical hot steel particles on powdered cellulose	<ul style="list-style-type: none"> Particles with diameters: 0.8–19.1 mm Particles temperature: 500–1300°C 	<ul style="list-style-type: none"> A significant relationship was found between particle size and temperature for ignition Increasing the particle temperature led to a decrease in the particle size required to sustain ignition
Suzuki et al. (2014)	The impact of continuous wind-driven firebrand showers on ignition of fuel bed attached to a non-combustible re-entrant corner assembly	<ul style="list-style-type: none"> Fuel bed sample: shredded hardwood mulch beds, measuring 1.2 m × 1.2 m × 51 mm thick. Wind speed: 6.0 and 8.0 m/s Moisture content: dried to 83% 	<ul style="list-style-type: none"> An inverse relationship between increasing wind speed and the number/mass of firebrands required to sustain ignition was found Notably, a wind speed of 8 m/s was able to sustain ignition of a fuel bed with moisture up to 83%
Ellis (2015)	Study on ignition of dry-eucalypt forest litter by standard flaming and glowing firebrands	<ul style="list-style-type: none"> Flaming firebrands were made of bamboo sticks 50 mm long Glowing firebrands were made of shed bark of <i>Eucalyptus</i>, with 50 mm long, 15 mm wide, and 2 mm in thickness Fuel bed sample: 400 × 400 mm with MC between 4 and 21% Wind speed: 0, 1.0, 2.0 m/s 	<ul style="list-style-type: none"> Ignition probability was sensitive to variation in fuel moisture content and wind conditions
Filkov et al. (2016)	Interaction of smouldering pine bark firebrands with surface litter (pine needle) fuel beds	<ul style="list-style-type: none"> Firebrands size: 10 × 10, 15 × 15, 20 × 20, 25 × 25, 30 × 30 mm² Wind speed: 1.0, 1.5, 2.0, 3 m/s 	<ul style="list-style-type: none"> Fewer larger firebrands were required to sustain ignition A firebrand with size of 10 × 10 mm² was unable to initiate ignition of the fuel bed An increase in the flow rate led to an increase in the probability of fuel bed ignition and reduction in the particle size
Matvienko et al. (2018)	A 3D mathematical model to simulate the ignition of fuel beds by glowing firebrands	<ul style="list-style-type: none"> Firebrand type: pine bark (10 × 10 to 30 × 30 mm²) and pine branches (2 mm < d < 8 mm). Fuel bed density range: 60–105 kg/m³ Airflow velocity: ≥2 m/s Firebrand temperature: ≤1073 K 	<ul style="list-style-type: none"> The firebrand length had a significant impact in the initiation of ignition
Fang et al. (2021)	Interaction of the coupled action of a hot metal particle and thermal radiation with a pine needle fuel bed	<ul style="list-style-type: none"> Particle diameter: 8, 10, 12 mm Particle temperature: 700–1100°C (step: 50°C) Radiation heat flux: 5–30 kW/m² No wind; ambient temperature: 20°C 	<ul style="list-style-type: none"> Inverse relationship between radiant heat flux and both particle diameter and temperature The critical radiant heat flux required for sustained ignition was 17.76 kW/m² when the ignition probability reached 50% Ignition delay time decreased as radiation heat flux increased

(Continued on next page)

Table 3. (Continued)

Ref.	Study conditions	Study parameters	Findings
Suzuki and Manzello (2021d)	Study of the ability to ignite adjacent wall assemblies with different separation distance by continuous wind-driven firebrand showers	<ul style="list-style-type: none"> Fuel bed type: shredded hardwood, Japanese cypress, pine bark nuggets, mini pine bark nuggets Wind speeds: 6, 8 m/s Separation distance: 102, 203 mm 	<ul style="list-style-type: none"> The significant gaps between the particles of pine bark nuggets reduced their susceptibility to ignition A higher risk of susceptibility of ignition of the adjacent wall assemblies by the fuel bed was observed with Japanese cypress and mini pine bark nuggets
Wessies and Ezekoye (2022b)	Using thermocouple and IR camera measurements to observe the growth of the reacting area between a firebrand and a fuel bed to predict ignition	<ul style="list-style-type: none"> Fuel bed sample 320 × 490 × 40 mm Flow conditions: Ujet = 0.63, 1.62 m/s Cylindrical firebrands: 19.2 diameter, 11 mm height 	<ul style="list-style-type: none"> Firebrand temperature and fuel bed temperature data were insufficient to predict ignition A quantitative definition of ignition was found, defined as the temperature of the reacting area in the fuel bed surpassing 500°C
Suzuki and Manzello (2021b, 2023)	Coupled effect of radiative heat flux and firebrands on the ignition of a fuel bed	<ul style="list-style-type: none"> Firebrand mass flux: 20, 40, 60 g/min Radiant heat flux: 5.8 kW Pre-heating times: 0, 600, 1200 s Wind speed: 4.0, 6.0, 8.0 m/s 	<ul style="list-style-type: none"> Radiative heat flux played a significant role in ignition time at wind speed 6 m/s but had little effect at 8 m/s owing to the increase in convective cooling Notably, the mass flux of firebrands required to achieve ignition decreased with increased pre-heating time

Ignition by individual natural firebrands

Different factors affect the ignition process when firebrands interact with a fuel bed. These factors include the characteristics of the firebrands, the properties of the fuel bed and the environmental conditions. These factors collectively determine the potential and speed of fuel bed ignition, which are discussed in the following sections.

Influence of firebrand characteristics

The shape and material of the firebrands play a key role in their thermal contact, burning temperature and duration, subsequently affecting their impact on the fuel bed (Bearinger *et al.* 2021b; Wong *et al.* 2022). Larger firebrands have a larger mass and carry more heat energy, allowing them to transfer sufficient energy to the fuel bed to heat, pyrolyse and ignite it compared with smaller ones (Salehizadeh *et al.* 2021; Manzello and Suzuki 2023; Matvienko *et al.* 2023). Smaller firebrands exhibit different behaviour. Their smaller size allows them to penetrate more deeply into the fuel bed, particularly when the bed has large pores and a low packing ratio. This deeper penetration enables smaller firebrands to become embedded within the fuel, potentially igniting it from the inside, even though they carry less energy than larger firebrands (Hernández *et al.* 2018; Yang *et al.* 2022). For instance, researchers Manzello *et al.* (2005a, 2006a) investigated the ignition vulnerability of various fuel bed types using two different sizes of disc-shaped firebrands. One set of firebrands had dimensions of 25 mm diameter and 8 mm thickness, while the other had 50 mm diameter and 6 mm thickness. The study

considered both smouldering and flaming single firebrands under applied wind speeds of 0.5 and 1 m/s. The results showed that a single smouldering firebrand does not have the ability to sustain ignition in any fuel bed type. In contrast, flaming firebrands consistently resulted in ignition in all cases. A similar trend was observed in the extended work of Manzello *et al.* (2008a), despite variations in firebrand geometry. Their study, which used cylindrical firebrands 10 mm in diameter and 76 mm in length, as well as 5 mm in diameter and 51 mm in length, reinforced the observation that a single smouldering firebrand alone was insufficient for ignition. These findings highlight the critical role of a firebrand's state of combustion on landing in determining ignition success. Additionally, Filkov *et al.* (2016) explored the impact of different-size cuboid pine bark firebrands, measuring 10 × 10, 15 × 15, 20 × 20, 25 × 25 and 30 × 30 mm² with a thickness of 5 mm, on the ignition of a pine needle litter fuel bed with a density of 105 kg/m³ and found that all firebrands were unable to initiate smouldering or flaming ignition of the fuel bed except for the 30 × 30 mm² firebrands.

Advanced computational modelling, which combines combustion and heat transfer principles, has provided valuable insights into the dynamics and the role of firebrands in the ignition process of fuel beds. For example, Waley (2018) proposed a heat transfer model to study the influence of thermal contact between glowing firebrands and the fuel bed using two different configurations: disc-shaped and cylindrical firebrands under the effect of wind speed. His results indicate that an increase in the contact pressure between the firebrand and the fuel bed led to higher

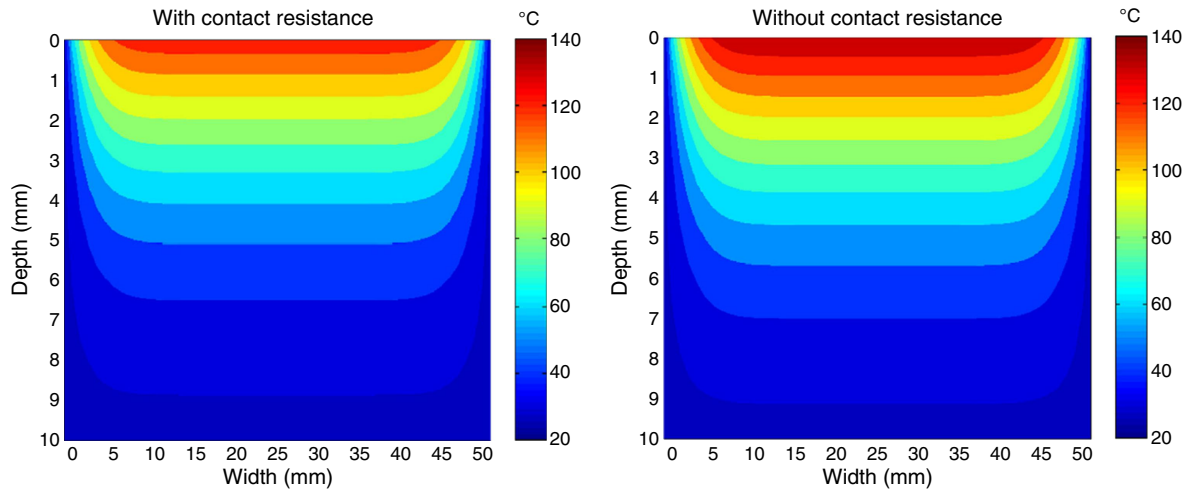


Fig. 10. Impact of thermal contact resistance on temperature patterns within a fuel bed (Warey 2018) (with permission from Elsevier, licence no. 5804610461534).

temperatures and greater thermal penetration depth within the target fuel bed, as shown in Fig. 10. Furthermore, the cylindrical firebrands exhibited a higher temperature in the fuel bed compared with the disc-shaped firebrands owing to their enhanced radiation heat transfer.

Other studies have incorporated more advanced modelling techniques, considering gas-phase reactions coupled with both a heat transfer model and a pyrolysis model to simulate the ignition process of the fuel bed by firebrands. These investigations enabled researchers to capture the complex interactions between the firebrands and the recipient fuel bed during ignition, providing a more comprehensive understanding of how heat transfer and pyrolysis influence the ignition behaviour of the fuel bed under various conditions. For example, a 3D mathematical model was employed in Matvienko *et al.* (2018) to simulate the ignition of fuel beds with different bulk densities and moisture contents under varying wind speed by glowing firebrands of different sizes. The results showed that increasing the length and diameter of the firebrands had a significant effect on initiating fuel bed ignition and reduced the ignition time. Furthermore, in Lautenberger and Fernandez-Pello (2009), a 2D numerical model was developed to simulate the ignition of a porous fuel bed (powdered cellulose) by glowing firebrands. This model handled the gas-phase reaction using fire dynamic simulations (FDSs) (McGrattan *et al.* 2013) and was coupled with a heat transfer and pyrolysis model to address condensed-phase phenomena. The study considered heat release rates of 4 and 6 MW/m³, with an applied airflow of 0.5 m/s. It was found that at the 4 MW/m³ heat release rate, only minimal smouldering occurred, resulting in the formation of a thin char layer near the fuel bed's surface. In contrast, at 6 MW/m³, considerable smouldering occurred. Yang *et al.* (2024) introduced a 2D computational model alongside bench-scale experiments to examine the glowing combustion behaviour of a wooden ember on a

non-reacting substrate. They utilised a global char oxidation reaction to simulate the combustion process. The findings demonstrated that increased airflow enhances ember combustion by supplying more oxygen, influencing heat transfer and altering combustion dynamics between embers and surfaces.

Influence of fuel bed characteristics

Influence of moisture content. The moisture content of the fuel bed plays a pivotal role in determining its likelihood of ignition by firebrands (Jervis and Rein 2016a; Revecó *et al.* 2024). Generally, fuel beds with lower moisture content are more prone to ignition by firebrands, as they require less energy to evaporate the water content within the fuel bed and have shorter ignition delays compared with those with higher moisture contents (Sun *et al.* 2018; Reszka *et al.* 2020). For instance, Urban *et al.* (2019a) conducted a series of experimental investigations to evaluate how the moisture content of a fuel bed influences smouldering ignition. These experiments were carried out in a small-scale wind tunnel, where they tested the ignition of a fuel bed made of coastal redwood sawdust by glowing firebrands. These firebrands were made by cutting birch, softwood and red oak dowel rods into cylinders with diameters ranging in size from 1.6 to 16 mm. The moisture content of the fuel varied from 0 to 50%, with some tests including a moisture content up to 70%. They found that ignition could occur at a maximum fuel moisture content (FMC) of 40%. They also noted that for larger firebrands, those with diameters greater than 11 mm, the probability of smouldering ignition depended more significantly on variations in FMC than on the size of the firebrands.

These observations align with studies examining the ignition probability and ignition delay time of various Mediterranean fuel beds, which found a notable inverse relationship between moisture content and ignition probability (Ganteaume *et al.* 2009; Viegas *et al.* 2014). These

studies also confirmed that as moisture content increased, ignition probability decreased and ignition delay time increased. Further, [Ganteaume et al. \(2009\)](#) extended their analysis to highlight the key role of moisture content on fire behaviour parameters such as fire spread, combustion rate and flame height, which showed a reduction in these parameters with higher moisture content. Further exploration of the relationship between moisture content and ignition behaviour was provided by [Yin et al. \(2014\)](#), who derived a new correlation for pine needle beds exposed to glowing firebrands under a controlled wind speed of 3 m/s. They observed that the square root of ignition time ($\sqrt{t_{ig}}$) presents a linear relationship with moisture content (MC), offering a relationship to predict the moisture content and ignition delay time as a function of fuel moisture (MC).

Influence of fuel bed arrangement and type. The type of fuel bed, particularly its particle size and the porous or solid nature of the fuel bed, significantly affects the ignition process ([Bean and Blunck 2021](#)). Generally, smaller particle sizes enhance the ignition process owing to their higher surface area-to-volume ratio, which facilitates better heat transfer and faster heating of the fuel, increasing its potential for ignition ([Urban et al. 2018](#)). Additionally, smaller particles also facilitate air penetration and oxygen access, further supporting the ignition and combustion processes ([Qin et al. 2024](#)). For instance, [Bean and Blunck \(2021\)](#) examined how fuel bed characteristics, particularly particle size and the difference between porous and solid fuel beds, influence ignition behaviour when exposed to a cartridge heater simulating a real firebrand. The experiments utilised Douglas-fir shavings with varying particle sizes ($L_c < 1$ mm, 4 mm $< L_c < 6$ mm, 6 mm $< L_c < 12$ mm), as well as Douglas-fir and cardboard plates. The results indicated that smaller particles in porous beds ignited more readily, whereas larger particles were more likely to ignite after

extended times as fewer particles came into contact with the heater, reducing the overall contact area.

Moreover, the packing ratio or bulk density, which indicates the density and porosity of the fuel bed, plays a key role in the ignition process ([Campbell-Lochrie et al. 2021](#); [He et al. 2021](#)). A higher packing ratio can enhance heat transfer between fuel bed particles, facilitating ignition, but may also restrict airflow and reduce oxygen availability. Conversely, a lower packing ratio may improve air circulation but could result in slower heat transfer and delayed ignition ([Qin et al. 2024](#)). For instance, [Kasymov et al. \(2016\)](#) conducted a series of experiments to investigate how the bulk density of the fuel bed influences the likelihood of ignition. They found that low porosity prevents firebrands from penetrating the fuel bed layer, resulting in significant energy loss to the surrounding environment during heat exchange, with only a small amount of energy reaching the fuel bed. Consequently, a higher fuel bed density reduced the probability of ignition. Additionally, fuel bed bulk density was recognised as a key factor affecting ignition delay time and flammability characteristics including fire spread, combustion rate and flame height, with these parameters decreasing as bulk density increased ([Ganteaume et al. 2009](#)). Other studies focused on determining the ignition delay time and observing the ignition likelihood of forest fuel beds with varied packing ratios and bulk densities ([Ganteaume et al. 2009](#); [Viegas et al. 2014](#); [Yin et al. 2014](#)). An increase in the time to ignition with increasing fuel bed bulk density was observed. In contrast, as shown in [Fig. 11](#), an increase in the packing ratio of the fuel bed significantly decreased the ignition delay time of the fuel bed ([Hernández et al. 2018](#); [Rivera et al. 2020](#)).

Other studies have consistently highlighted the significant influence of fuel bed type exposed to firebrands on ignition success. Experimental studies ([Ganteaume et al. 2009](#); [Viegas et al. 2014](#)) investigating the ignition

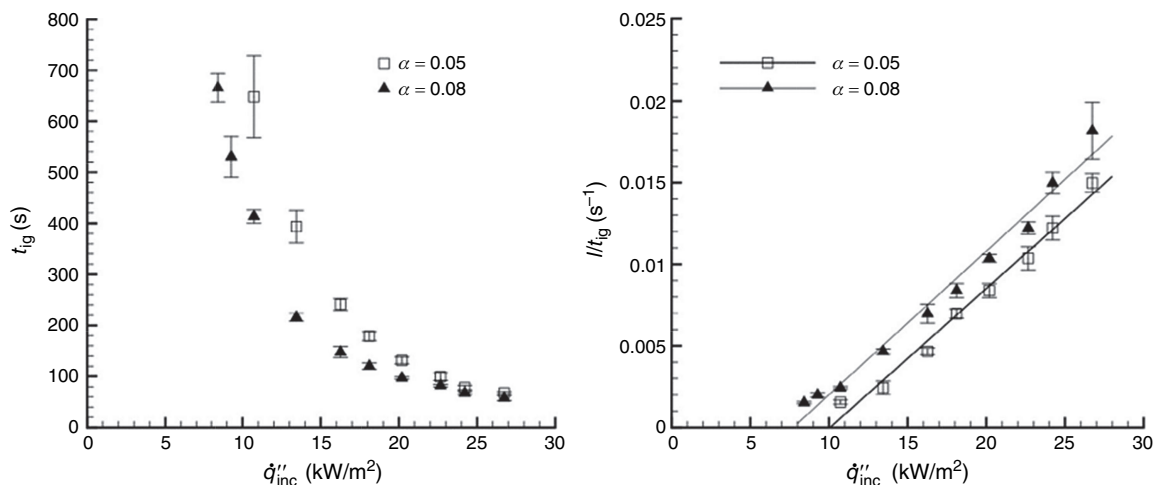


Fig. 11. The effect of the pine needle fuel bed packing ratio (α) on ignition delay time using an electrical heater to represent an idealised firebrand ([Hernández et al. 2018](#)) (with permission from Elsevier, licence no. 5820010199496).

probability and ignition time delay of various Mediterranean fuel beds when exposed firebrands observed that pine needles exhibited the highest ignition probability and the shortest ignition delay, whereas eucalyptus leaves had the lowest ignition probability. Additionally, it was noted that grass fuel beds were more flammable than litter fuel beds. These findings are aligned with the work of [Manzello *et al.* \(2008a\)](#), who reported that pine needles and shredded paper readily ignited when exposed to single flaming firebrands, whereas shredded mulch beds demonstrated higher resistance to ignition. These observations suggest that fine, loosely packed fuels such as pine needles and grass promote rapid ignition owing to their high permeability, which enhances oxygen availability, a key role in sustaining ignition. In contrast, denser and more compacted fuels are more resistant to ignition owing to their reduced permeability, which limits oxygen diffusion and the ignition process.

Influence of wind speed. Environmental conditions such as wind, temperature and humidity have a considerable role in the ignition of a receptive fuel bed by firebrands. Increasing the wind speed enhances the oxidation of these firebrands and raises their surface temperature, influencing pre-heating and thermal degradation of the fuel bed, thus increasing its ignition probability ([Atreya and Abu-Zaid 1991](#); [Yan *et al.* 2024](#)). For instance, [Ellis \(2011, 2015\)](#) demonstrated the effect of environmental conditions, specifically the influence of wind speed, on the likelihood of ignition of dry eucalypt forest litter by firebrands. It was observed that flaming ignition of the fuel bed occurred in windy conditions, whereas smouldering occurred in quiescent air conditions. Similarly, [Manzello *et al.* \(2006a, 2008a\)](#) reported that airflow is crucial for successfully achieving flaming ignition in a fuel bed.

Additional experiments demonstrated that wind speed plays a key role in supplying oxygen to the firebrand surface, thereby enhancing its oxidation, increasing heat release and accelerating the ignition of surface litter ([Filkov *et al.* 2016](#); [Kasymov *et al.* 2016](#)). The authors noted that as wind speed increased, smouldering ignition and its transition to flaming required smaller particle sizes and fewer particles. Moreover, in [Yin *et al.* \(2014\)](#) and [Fang *et al.* \(2023\)](#), a significant relationship between wind speed and ignition delay time was observed, indicating that the time required to sustain ignition of a fuel bed decreased with an increase in wind speed, as shown in [Fig. 12](#). Additionally, [Ganteaume *et al.* \(2009\)](#) found that airflow and its direction relative to firebrands played a crucial role in determining ignition time, regardless of the fuel bed's MC. Their study revealed that oblique airflow ($\sim 45^\circ$ to the fuel bed) accelerated ignition by improving oxygen supply to the firebrand and enhancing heat transfer within the fuel bed, while minimising heat loss compared with horizontal airflow, which resulted in a considerably longer ignition time. [Yin *et al.* \(2014\)](#) observed that pine needles could be ignited by

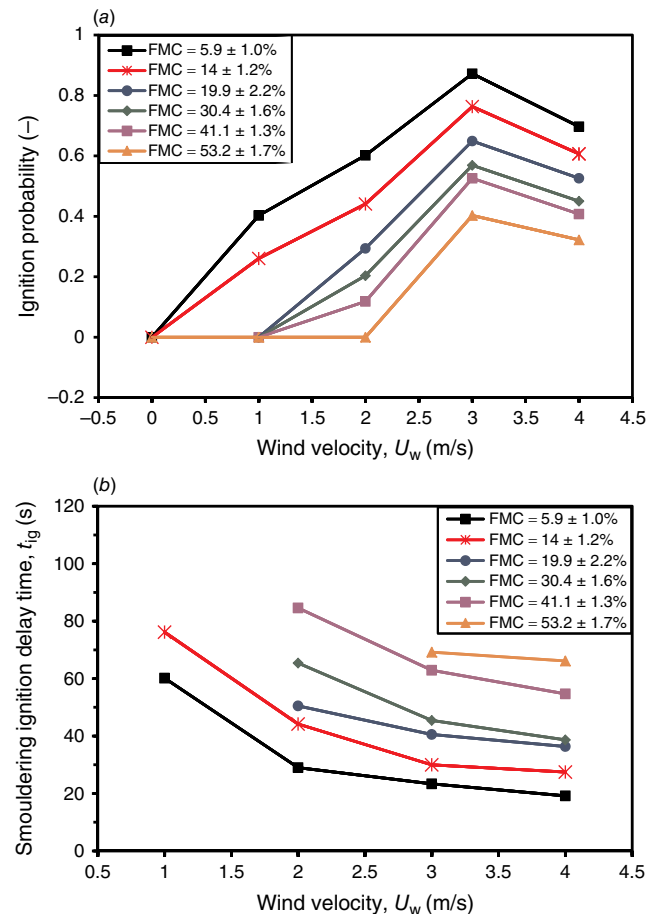


Fig. 12. The effect of wind speed and moisture content on (a) ignition probability, (b) and the ignition delay time of a moist pine needle fuel bed using a cubic-shaped (2 cm^3) firebrands made of spruce (produced from data in [Fang *et al.* 2023](#)).

a glowing firebrand even when the FMC was as high as 65% provided there was an airflow of 3 m/s.

Ignition by hot metal particles

Despite the complexity of firebrands in wildfires and the effect of environmental conditions on their shape, mass and size and the formation of an ash layer on the outer surface of the char core affecting oxidation and combustion processes, researchers have sought to simplify their behaviour by using hot metal particles as surrogates for firebrands in their investigations ([Zak *et al.* 2013](#); [Wessies and Ezekoye 2022a](#); [Wang *et al.* 2024](#)). This approach allowed control of the thermal and physical properties of firebrands, including temperature, size and heating effects on various fuel beds. For example, [Wang *et al.* \(2017\)](#) investigated the probability of ignition in a forest fuel bed made of pine needles with varying MC (ranging from 6 to 32%) and under applied wind speeds of 0–4 m/s using stainless steel particles (6–8 mm diameter, 600–1100°C). Their results, shown in [Fig. 13](#), indicated that flaming ignition time decreased with higher particle temperature and

wind speed, whereas it increased with higher fuel bed MC. Comparatively, Wang *et al.* (2025) further examined the ignition behaviour of WUI fuels (pine needles, straw and cotton) under quiescent conditions, using larger stainless-steel particles (12 mm diameter) with both solid and hollow particles (void ratios of 0, 0.59 and 0.68). Notably, their study highlighted that cotton was the most easily ignited, requiring the lowest particle temperature and exhibiting the fastest flame spread. In contrast, straw was the most resistant to ignition, requiring a minimum temperature of 950°C for flaming ignition. Additionally, the study found that hollow particles lowered the ignition threshold for cotton by extending contact time but inhibited smouldering ignition across all fuels owing to rapid cooling.

The effect of the size and temperature of hot metal particles on ignition was also investigated in Hadden *et al.* (2011), Scott *et al.* (2011) and Urban *et al.* (2017). A crucial finding from these investigations was the inverse relationship between the size of the particles and the temperatures necessary for either smouldering or flaming ignition, revealing that smaller particles require a higher temperature to produce either smouldering or flaming ignition of the fuel bed compared with larger particles. However, in contrast to the previous studies that focused exclusively on stainless steel and steel particles, the studies of Zak *et al.* (2014), Fernandez-Pello *et al.* (2015) and Urban *et al.* (2015) expanded this work to assess the effect of thermal properties, such as specific heat and thermal conductivity, on ignition behaviour. This included investigations of stainless steel, aluminium, brass and copper hot particles. Most materials were found not to have a significant influence on ignition;

however, copper was an exception owing to its significantly higher thermal conductivity and thermal diffusivity, which are at least three times greater than those of the other materials. Fang *et al.* (2021) adopted a different approach by investigating the combined effect of hot metal particles and thermal radiation on the ignition of a pine needle fuel bed. They used a resistive heating cone measuring $10 \times 10 \text{ cm}^2$, positioned 2.5 cm above the fuel bed to act as a thermal radiation source. As shown in Fig. 14, their results indicated that with an increase in particle temperature, diameter and radiant heat flux, flaming ignition was observed and the ignition probability increased. Finally, the experimental results revealed that the ignition delay time decreased as radiative heat flux increased.

Other studies employed an electrical heater to simulate an ideal firebrand to study the ignition of porous fuel beds (Hernández *et al.* 2018; Rivera *et al.* 2020; Bean and Blunck 2021; Álvarez *et al.* 2023). In these studies, researchers varied the fuel bed packing ratio and heater temperature to assess their impact on ignition likelihood. Increasing both the heater temperature and the fuel bed packing ratio resulted in a higher ignition probability and a reduced ignition delay time.

Ignition by accumulated firebrands

The heat generated by a firebrand pile is expected to vary from that of a single firebrand owing to the interaction among the firebrands within the pile. The interaction between individual firebrands in the pile is expected to change the heat transfer processes involved in the ignition

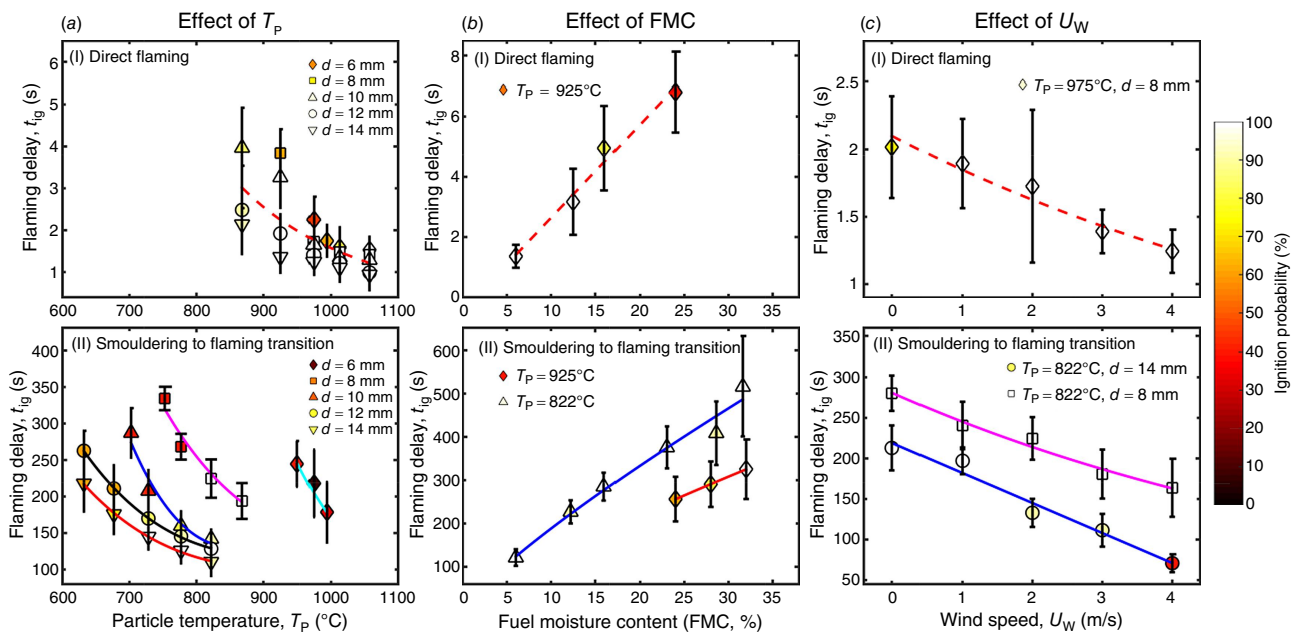


Fig. 13. Impact of particle (a) diameter, and temperature, (b) fuel bed moisture content and (c) wind speed on the ignition delay time of a pine needle fuel bed (Wang *et al.* 2017) (with permission conveyed through Copyright Clearance Center, Inc., licence ID: 1492644_1).

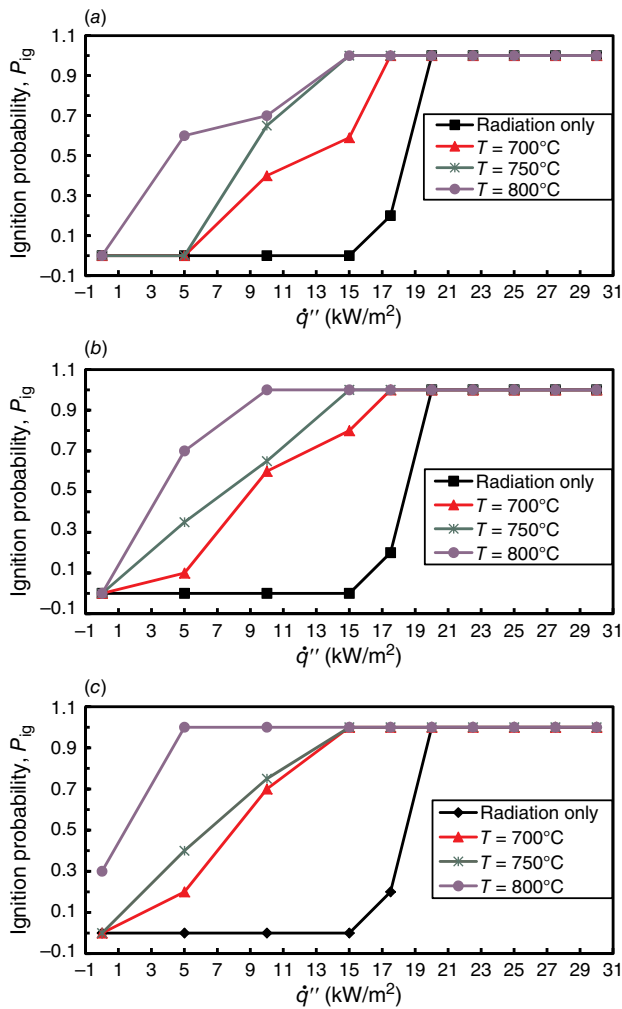


Fig. 14. The effect of thermal radiation (\dot{q}'') coupled with a hot particle on the ignition probability of a pine needle fuel bed with a moisture content of 5.17% and particle diameter of: (a) $d_p = 8$ mm, (b) $d_p = 10$ mm, and (c) $d_p = 12$ mm (produced from data in Fang et al. 2021).

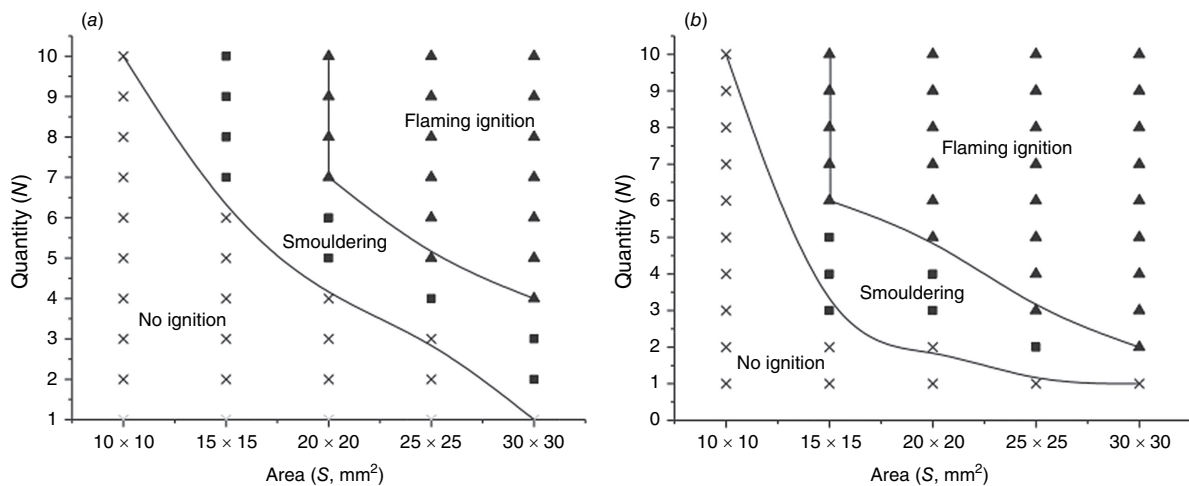


Fig. 15. The effect of the number of accumulated firebrands of varying sizes made from pine bark on the ignition of pine needle surface litter with a moisture content of 9.3% under wind speeds of: (a) 1.5 m/s, and (b) 2.0 m/s (Filkov et al. 2016).

of solid fuels when exposed to a pile of firebrands (Kasymov et al. 2018). The accumulation of multiple firebrands in a pile can serve to retain heat for an extended period, thereby enhancing the chances of smouldering ignition in fuel beds, which may then transit to flaming ignition. As the number or mass of firebrands increases, the heat flux to the fuel bed intensifies, as discussed in the ‘Thermal behaviour of firebrands’ section, reducing the time to ignition and increasing the likelihood of a fire transitioning from a smouldering to a flaming state. For instance, Manzello et al. (2005b, 2006a) demonstrated that multiple glowing firebrands have the potential to not only initiate smouldering ignition but also transition to flaming ignition. This observation aligns with Kasymov et al. (2018), who highlighted the role of firebrand accumulation in sustaining ignition in fuel beds. Additionally, Manzello et al. (2006b) further expanded our understanding about the influence of firebrand accumulation in sustaining ignition in a pine needle fuel bed by identifying the minimum firebrand mass required to sustain ignition. They found that for flaming firebrands, a minimum mass of 1 g was sufficient to sustain flaming ignition. In contrast, a significantly higher mass of 6 g was required to achieve a sustained smouldering ignition that could eventually transition to flaming under an airflow of 1 m/s.

Furthermore, the study by Filkov et al. (2016) presented a relationship between the accumulation of glowing firebrands and both smouldering and flaming ignition of a fuel bed. Fig. 15 shows that as the number of accumulated glowing firebrands increases, the likelihood of smouldering and flaming ignition increases. The effect of another critical factor, airflow temperature, on the minimum accumulated firebrand mass required to sustain ignition was explored by Kasymov et al. (2016). It was noted that an increase in the ignition probability and a decrease in the number and size of firebrands required to sustain ignition occur with an increase in air flow temperature.

A more recent study by Lin *et al.* (2024a) provides further insights into how firebrand pile mass and wind speed influence ignition dynamics. They performed a series of experiments in a small-scale wind tunnel to examine the smouldering ignition and transition to flaming of four mulch types (black mulch, forest floor, redwood and fir bark) when exposed to glowing firebrand piles under wind speeds up to 1.4 m/s. The firebrand pile masses ranged from 0.06 to 0.79 g. Notably, they observed that as the mass of the firebrand piles increased, the minimum wind speed needed for smouldering ignition decreased. Additionally, the transition from smouldering to flaming occurred at a critical wind speed, which was unaffected by the firebrand pile mass but varied depending on the mulch type, as shown in Fig. 16. Moreover, they found that a critical surface temperature of approximately 850°C was necessary for the smouldering to flaming transition.

Ignition by firebrand showers

Firebrand showers are characterised by a dynamic and transient process in which individual firebrands remain airborne and influence ignition during their period of flight

(Manzello and Suzuki 2023). In contrast, accumulated firebrands (piles) represent a static phase, forming when multiple firebrands land in one location. Whereas firebrand piles are significant for localised ignition and prolonged combustion owing to their ability to smoulder and retain heat for extended durations, firebrand showers present a different challenge. These showers consist of thousands of small particles that can be carried by strong winds over significant distances, bypassing firebreaks and natural barriers to ignite new fires far from the main fire front (Quarles and Standohar-Alfano 2018). The development of the firebrand generator shown in Fig. 17 by the National Institute of Standards and Technology (NIST) has significantly advanced knowledge about firebrand showers. It has allowed researchers to investigate the ignition potential of various natural fuel beds and structural components under exposure to firebrand showers (Manzello *et al.* 2008b). The firebrand generator allows the control of firebrand characteristics such as mass and number flux.

Firebrand showers have been extensively studied to understand their influence on the ignition of natural fuel beds. Researchers have focused on the critical role these

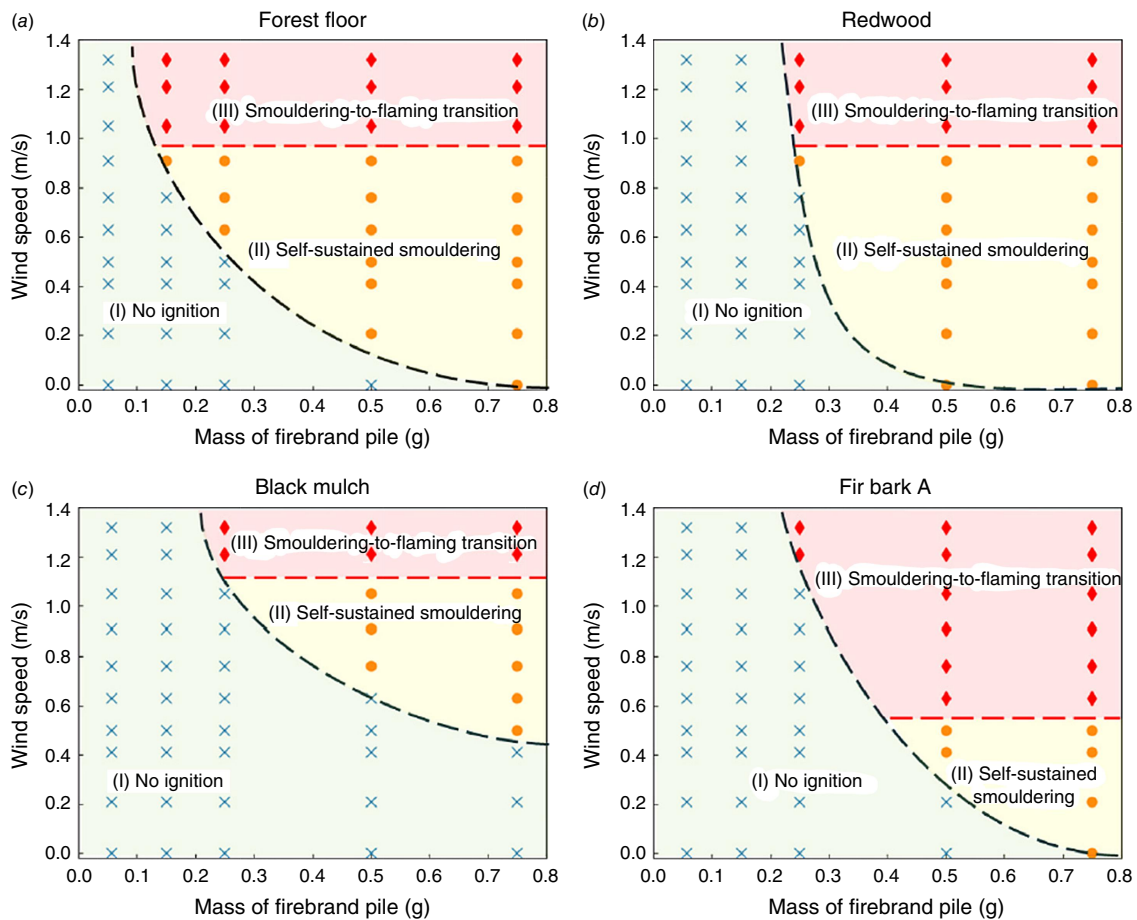


Fig. 16. Critical conditions for smouldering ignition and its transition to flaming of different mulch samples, (a) forest floor, (b) redwood, (c) black mulch, and (d) fir bark A under different wind speeds and masses of firebrand pile (Lin *et al.* 2024a).

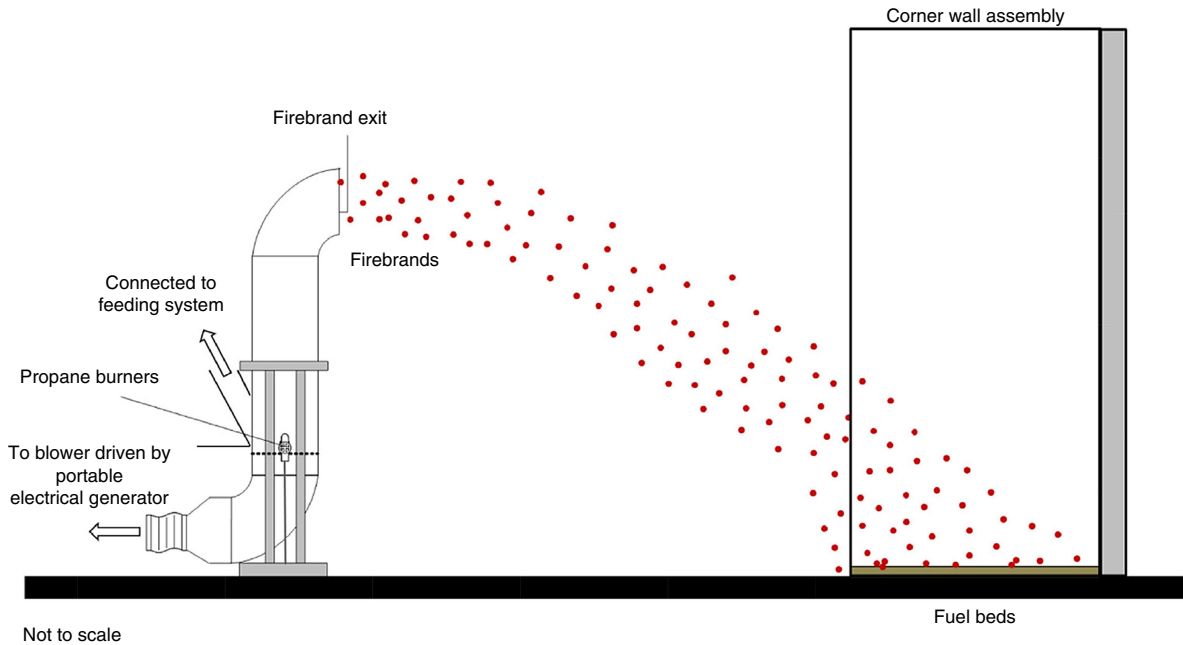


Fig. 17. Schematic diagram of the firebrand generator developed by NIST (Suzuki and Manzello 2020b) (with permission from Elsevier, licence no. 5805060146603).

firebrands play in the spread of fires, particularly in WUI areas. For example, laboratory experiments were conducted to assess the ignition of mulch beds by continuous firebrand showers under applied wind speeds of 6 and 8 m/s (Manzello *et al.* 2017; Suzuki and Manzello 2021a, 2021d). Douglas-fir wood particles, cut into $7.9 \times 7.9 \times 12.5$ mm size, were used as firebrands in these experiments. Four different mulch fuel beds made of shredded hardwood mulch, Japanese cypress woodchip mulch, pine bark nuggets and mini pine bark nuggets were tested. The results indicated that at a wind speed of 6 m/s, the firebrands were capable of igniting all the mulch fuel beds except for the pine bark nuggets. The lack of ignition in the pine bark nuggets is due to significant gaps between its fuel particles, which result in increased heat transfer from the firebrands to the surrounding environment rather than directly to the fuel bed. Additionally, increasing the firebrand flux and the number of firebrands had a significant impact on decreasing ignition time.

Additional laboratory studies by Suzuki *et al.* (2014) and Suzuki and Manzello (2020b) were conducted to assess the time to ignition, the effect of MCs ranging from dry up to 83%, and wind speeds varying from 6 to 8 m/s, as well as the number of firebrands landing on a hardwood shredded mulch fuel bed measuring $1200 \times 1200 \times 51$ mm. The results, shown in Fig. 18, indicate that under a wind speed of 6 m/s, firebrands were able to sustain smouldering, which subsequently transitioned to flaming ignition when the fuel bed's MC ranged between 40 and 60%. However, at a higher wind speed of 8 m/s, this moisture threshold increased to 86%, indicating that higher airflow can facilitate ignition even in very wet fuel conditions. Moreover, it is notable that

a fuel bed with a higher MC requires a greater number of firebrands and more time to sustain ignition.

Suzuki and Manzello (2023) further expanded their analysis to examine the influence of the combined effect of radiation and firebrand showers on the ignition of cellulose fuel beds under varying wind speeds. Firebrands were fed in the generator at varying rates of 20, 40 and 60 g/min and wind speeds were set at 4, 6 and 8 m/s. A 5.8 kW radiant panel measuring 300×300 mm at a height of 440 mm above the cellulose fuel bed was used. Additionally, different pre-heating times, varying across 0, 600 and 1200 s after the firebrand generator was started were tested. The results revealed that the higher feeding rates, wind speeds and pre-heating times yielded a higher probability of fuel bed ignition. Moreover, higher wind speeds required a lower number of firebrands for fuel bed ignition owing to the enhanced firebrand combustion process resulting from a higher rate of oxidiser supply. Similarly, in Suzuki and Manzello (2021b), the authors found that the heat flux generated by the radiant panel had a significant impact on reducing the time required and number of firebrands needed to sustain both smouldering and flaming ignition when the wind speed was set at 6 m/s. However, this effect was less notable when the wind speed was increased to 8 m/s.

Knowledge gaps

Most research on the ignition of natural fuel beds by firebrands has been conducted in laboratory studies. In these studies, researchers have investigated different parameters such as firebrand and fuel bed characteristics, as well as environmental conditions, to explore the role of

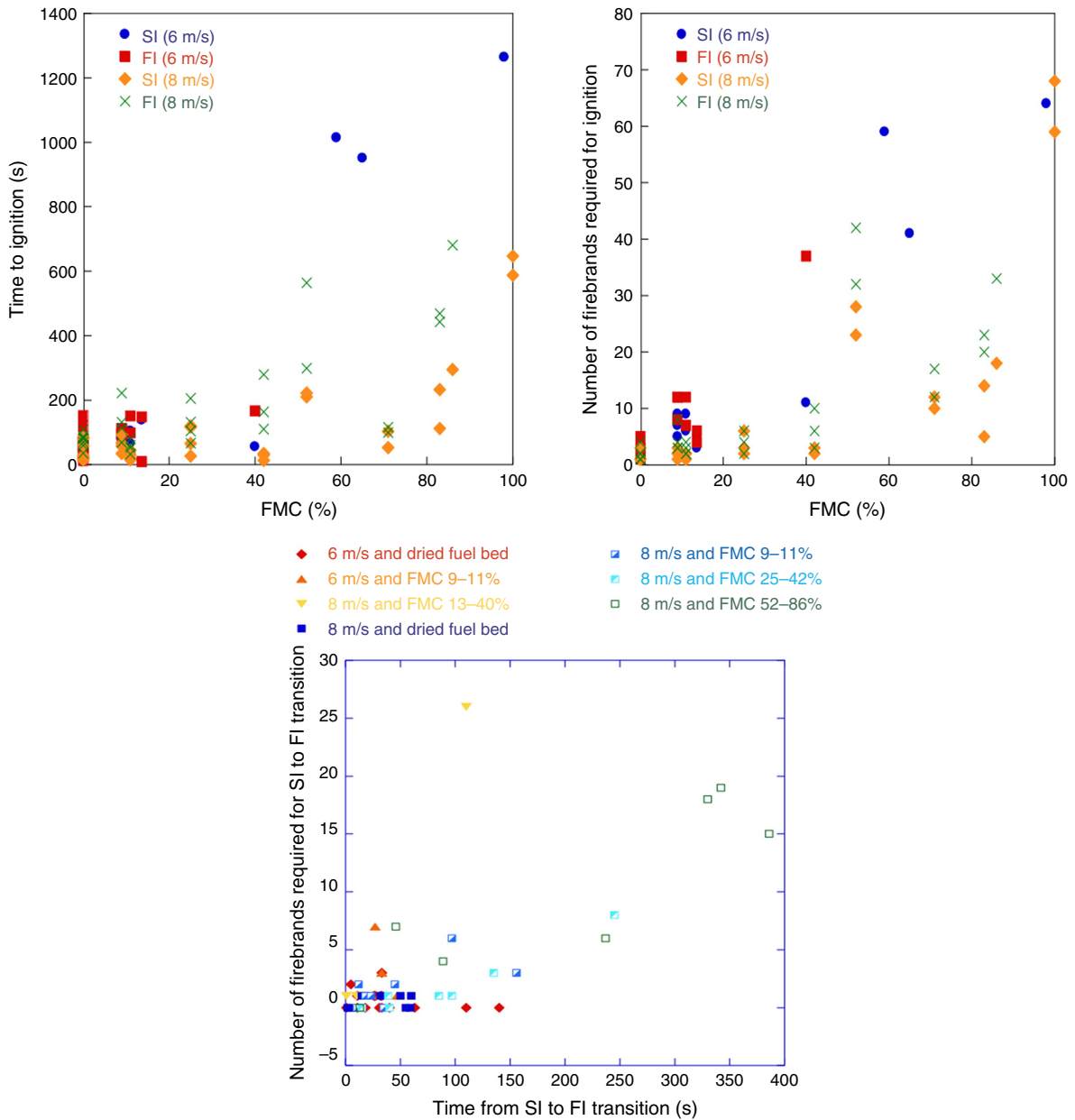


Fig. 18. The minimum number of firebrands required to sustain ignition of a hardwood shredded mulch fuel bed exposed to wind-driven firebrand showers under various wind speed and moisture contents (Suzuki and Manzello 2020b) (with permission from Elsevier, licence no. 5805060146603). Note: SI is smouldering ignition, and FI flaming ignition.

firebrands in fuel bed ignition and the spread of spot fires. It was found that flaming firebrands have enough energy to pre-heat and ignite higher MC fuel beds compared with glowing firebrands. The shape and size of firebrands significantly influenced the likelihood of fuel bed ignition. Larger firebrands tended to carry more energy and burn for a longer duration, increasing the chance of igniting the fuel bed on contact. Additionally, the type of fuel, MC and bulk density played critical roles in the fuel bed ignition potential. In general, fuel beds with lower MC ignite more quickly because they require less energy from the firebrands to dry

and pre-heat fuel to their ignition temperature. A negative relationship was found between wind speed and firebrand mass and number flux.

Despite considerable research efforts into the thermal degradation and ignition processes of vegetative fuel beds by firebrands in the WUI, most studies have focused on specific configurations and parameters, limiting a broader understanding of the phenomenon. These investigations have identified critical thresholds for factors such as fuel bed MC, wind velocity and firebrand characteristics (e.g. size and shape) that affect ignition probability. However, a

significant gap remains in developing a more generalised theory applicable to a wider range of scenarios. For instance, critical moisture levels may vary significantly depending on the type of vegetation, environmental conditions (e.g. temperature and humidity), or duration of exposure to firebrands, making it difficult to generalise findings. Additionally, the interaction between firebrands and varying wind velocities often studied in laboratories may not fully capture the complexities of real-world conditions. Therefore, current knowledge is often limited to specific experimental conditions, posing challenges in applying these findings to the diverse fuel types, environmental conditions and firebrand properties encountered in real-world wildfires. Consequently, there remain significant gaps in understanding the chemical and thermal interactions between firebrands and the recipient fuel bed during spotting phenomena. Key knowledge gaps include: limited understanding of the residual potential energy of firebrands after flight and transport from the fire source and insufficient data on the impact of firebrand accumulation, their formation into piles, accumulation pattern, and role in the ignition mechanism of the receiving fuel bed. Although individual firebrands have been widely studied, their collective behaviour, especially when forming piles, presents additional complexities related to heat retention, oxygen supply, reradiation and convective heat transfer within the pile. Understanding these thermal interactions is essential as they play a key role in the ignition process of the receiving fuel bed.

Another significant gap is the lack of data on the combined effects of firebrand showers or firebrand accumulation with radiation and convection impact on ignition behaviour. Addressing these gaps by conducting field studies to explore firebrand behaviour in real fires could provide valuable insights to better understand the ignition process and spread of fires, which are challenging to replicate in laboratory settings. Moreover, developing computational models that simulate firebrand shower behaviour, accumulation, pile formation and their interaction with environmental factors is also essential.

Ignition of structures by firebrands

In communities situated at the WUI, not only vegetation but structures and man-made fuels themselves are susceptible to ignition by firebrands. These elements can be viewed as a fuel source. Once ignited, they may generate additional firebrands, thereby increasing the risk of fire spread throughout the community (Suzuki and Manzello 2019). The ignition of wood structures follows the same fundamental process described earlier in the 'Ignition of vegetative fuel beds by firebrands' section. However, the mechanisms through which firebrands ignite natural fuel beds and wood structures differ significantly owing to variations in their physical and thermal properties. Natural fuel beds, such as

leaves and grasses, typically have lower ignition thresholds owing to their fine structure and high surface-area-to-volume ratio, allowing rapid heat transfer and quicker ignition when exposed to firebrands. In contrast, wood structures, including decking and siding, generally require prolonged heating owing to their greater density and lower surface area-to-volume ratio, which affects heat penetration and delays ignition. Similarly to natural fuel, ignition of structural components is significantly affected by firebrand characteristics, material properties and configuration. These factors collectively determine the likelihood of structure ignition. This section reviews several aspects related to the influence of firebrands on building ignition, focusing on four critical areas: analysing how different materials and designs, along with firebrand characteristics, influence a building's ability to withstand firebrand attacks; understanding the impact of firebrand accumulation and firebrand showers on the likelihood of structural ignition; discussing methods for enhancing building resilience against firebrand attacks; and highlighting innovative design choices and materials that can reduce the risk of fire spread. A summary of the reviewed studies is presented in Table 4.

Influence of firebrand characteristics

Recently, there have been increasing efforts in scientific research aimed at examining the evolving role of firebrands in the ignition of the building structures. Various factors, including the size, quantity, mass and shape of the firebrands, as well as their accumulation pattern, significantly affect their potential to ignite structural materials (Suzuki and Manzello 2019; Wessies *et al.* 2019). For instance, studies (Kasymov *et al.* 2019; Tarakanova *et al.* 2020; Matvienko *et al.* 2022) evaluated factors such as firebrand size and quantity, as well as the presence of airflow on ignition probability and the ignition delay time in various construction materials. These studies consistently highlight the key role of wind speed in determining the likelihood of structure ignition by firebrands. Specifically, at wind speeds between 0 and 1 m/s, firebrands mostly smoulder without transitioning to flaming ignition. However, as wind speed increases, the ignition probability increases while the ignition time decreases for the same firebrand size and quantity. Notably, at higher wind speeds (2–2.5 m/s), larger firebrands significantly lower the minimum number of firebrands required to sustain ignition.

In contrast to the previous studies that mainly focused on wind speed and number of firebrands, Kwon and Liao (2022a, 2022b) systematically explored the impact of firebrand spacing to determine critical conditions for the ignition and burning of building materials. They demonstrated that when the spacing between firebrands exceeded 20 mm, the firebrands were only able to burn on the surface of plywood material until they were completely consumed. In contrast, spacing less than 20 mm led to conditions where

Table 4. Summary of studies on the ignition of structures by firebrands.

Ref.	Study conditions	Study parameters	Findings
Suzuki <i>et al.</i> (2016)	Ignition propensity of wooden face assemblies with and without nearby natural fuel sources	<ul style="list-style-type: none"> Wood assembly configuration: flat wall, inside corner, outside corner and V-corner Wood assembly dimension: $W \times H = 0.91 \times 0.91$ m, and 1.83×1.83 m Wood assembly material: cedar, redwood 	<ul style="list-style-type: none"> The presence of a natural fuel bed adjacent to the wooden face assemblies significantly influenced ignition propensity, as flaming was observed in all cases; in contrast, smouldering sometimes occurred without the natural fuel bed Redwood produced firebrands of larger size compared with cedar owing to ignition
Manzello and Suzuki (2019)	Experiments focused on understanding the impact of board spacing in decking assemblies on ignition behaviour	<ul style="list-style-type: none"> Wood assembly material: western red cedar, Douglas-fir, redwood Board spacing: 0, 5, and 10 mm 	<ul style="list-style-type: none"> Larger gaps allowed greater accumulation of firebrands, increasing ignition propensity
Meerpoel-Pietri <i>et al.</i> (2021)	Ignition propensity of decking slabs by flaming firebrands	<ul style="list-style-type: none"> Firebrand area: 0.07 and 12.00 cm² Firebrand mass: from 0.57 mg to 2.66 g Decking type: pine, thermoplastic 	<ul style="list-style-type: none"> A minimum mass of 0.31 and 0.80 g was required for pine and thermoplastic slab to initiate ignition, respectively A critical position of firebrand deposition was necessary to sustain ignition
Salehizadeh <i>et al.</i> (2021)	Interaction between a smouldering firebrand pile and woody fuel to quantify critical ignition conditions	<ul style="list-style-type: none"> Test sample: marine-grade plywood, oriented-strand board, cedar shingles Pile mass: 4.0, 8.0, and 16.0 g Wind speed: 0.5, 0.8, 1.2, 1.4 m/s 	<ul style="list-style-type: none"> Higher temperatures and heat flux were observed with increasing pile mass and wind speed, owing to reradiation between the particles and increasing rate of oxidation
Richter <i>et al.</i> (2022)	Analysing the influence of crevices in wooden material on ignition propensity	<ul style="list-style-type: none"> Firebrand mass: 10 g Firebrand bulk density: 0.061 g/cm³ Test sample configuration: flat, 0, 90° crevice configurations 	<ul style="list-style-type: none"> Crevice configuration samples received higher heat flux compared with flat configuration Crevices parallel to the air flow direction exhibited the highest ignition propensity, in contrast to crevices perpendicular to the air flow direction
Matvienko <i>et al.</i> (2022, 2023)	A series of experiments and 3D mathematical model to simulate wood ignition by firebrands	<ul style="list-style-type: none"> Wood material: plywood, oriented strand board, chipboard Firebrand size: $d = 6\text{--}8$ mm, $L = 40$ mm Wind speed: 0, 1 m/s 	<ul style="list-style-type: none"> Decreasing the distance between firebrands and increasing their length yielded higher ignition potential for wood samples
Zhu and Urban (2023)	Thermal interaction between an electrical heater acting as an idealised firebrand and a wood fuel bed	<ul style="list-style-type: none"> Heater size: 7.5, 15 mm Heat flux: 10–60 kW/m² Separation distance: 0 to 15 mm 	<ul style="list-style-type: none"> An inverse relationship between heater size and incident heat flux was observed in terms of ignition probability The separation distance had a significant role in the ignition delay time of the wood sample
De Beer <i>et al.</i> (2023a)	Influence of a glowing firebrand pile on the ignition of substrate materials	<ul style="list-style-type: none"> Coverage density: 0.06, 0.16 g/cm² Air velocity: 0.9, 1.4, 2.4, 2.7 m/s Substrate materials: Kaowool PM, western red cedar 	<ul style="list-style-type: none"> Increasing both air velocity and covering density had a significant impact on increasing propensity for ignition

the plywood not only ignited but also continued to burn even after the firebrands were consumed.

These observations are further substantiated by Zhu and Urban (2023), who experimentally and numerically investigated the effects of firebrand spacing using electrical heaters as real firebrands on the ignition of a wooden sample made of pine. As shown in Fig. 19, when the separation distance is large, a portion of the heat from the surface is used to heat the space between the two heaters, resulting in heat loss. Conversely, when the separation distance is small, the thermal interaction between the two firebrands compensates for this portion of heat loss, leading to higher ignition probability and shorter ignition delay times. Further, they expanded their

analysis to explore the effect of the heater size and heat flux, revealing that increasing both parameters enhanced ignition probability while reducing time to ignition.

Further explorations by Matvienko *et al.* (2023) employed a 3D mathematical model incorporating gas-phase reactions with a pyrolysis model to simulate the ignition of wood by firebrands. Although their findings on the importance of firebrand size and spacing are consistent with the previous studies, they uniquely highlighted the role of firebrand geometrical parameters. Specifically, they observed that closely spaced firebrands with larger sizes and greater lengths led to a high-temperature regime, generating sufficient thermal energy to initiate pyrolysis, eventually leading to ignition.

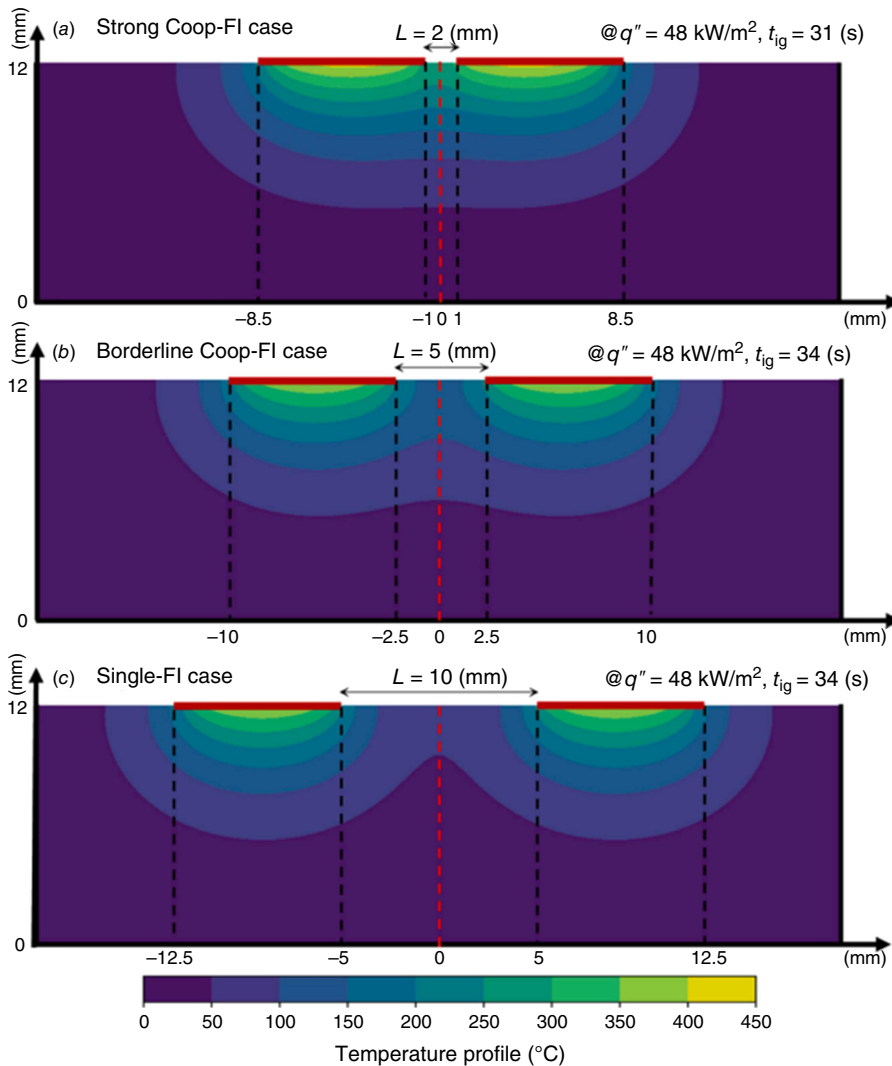


Fig. 19. The effect of separation distance: (a) 2 mm, (b) 5 mm, and (c) 10 mm between two electrical heaters representing idealised firebrands on the temperature profile of a wood sample (Zhu and Urban 2023) (with permission from Elsevier, licence no. 5820070271568). Note: cooperative flaming ignition (Coop-FI) was determined by comparing the ignition time difference when the fuel bed is exposed to either one or two firebrands. The cooperative flaming ignition (time) is defined as the difference between these two ignition times. The FI event was deemed a Coop-FI event if the ignition time in the two-heater case was 1 s smaller than that in an analogous single-heater case; otherwise, the outcome was treated as Single-FI. q = heat flux.

Although studies examining the ignition processes by multiple individual firebrands of structural materials attached at varying spacing distances and with different geometrical parameters have provided valuable insights into the susceptibility of structural components to ignition, these studies alone cannot provide a comprehensive assessment of the vulnerability of these components to ignition from the accumulated firebrands in the form of a pile (Dowling 1994). Post-fire investigations in the WUI have reported that firebrands carried over long distance by strong winds often accumulate in piles on various fuel surfaces before igniting them (Maranghides and Mell 2011; Manzello et al. 2020). These accumulated piles of firebrands store significantly more energy, posing a greater ignition hazard compared with individual firebrands. Factors such as ambient wind speed, firebrand pile mass, pile porosity and the density of target fuels contribute to the ignition potential of these piles. Firebrand pile porosity significantly influences the magnitude and duration of heat transfer from a firebrand pile, with higher-porosity piles exhibiting higher

velocities throughout the pile (Bearinger 2021). The interaction between firebrands within the pile enhances re-radiation among them, and the oxidation rate increases with higher wind speed. This intensifies the burning of the firebrands, consequently leading to higher temperatures and increased heat fluxes (Baldwin and Sunderland 2023; De Beer et al. 2023b).

One of the studies on the effect of firebrand pile accumulation on wooden structures was conducted by De Beer et al. (2023a), who examined how accumulation affected ignition in wooden structures by depositing firebrands onto both flammable (western red cedar) and non-flammable (Kaowool PM insulation) substrates. The firebrand pile measured 5×10 cm, with two distinct coverage densities of 0.06 and 0.16 cm². Airflow velocities ranged from 0.9 to 2.7 m/s. Their study revealed that both airflow velocity and firebrand coverage density significantly influence ignition, with the highest peak average back surface temperature of the substrate and heat release rate per unit area (HRRPUA) observed at an airflow rate of 2.4 m/s, although further

increases in airflow led to a decline in these parameters. Notably, they demonstrated that increasing firebrand coverage density enhanced the likelihood of ignition. [Lauterbach et al. \(2024\)](#) further expanded the previous study and highlighted the impact of firebrand pile orientation on ignition. They found that combustion was more intense when the 10-cm side of the firebrand pile was aligned with the airflow, indicating that pile orientation influences heat transfer dynamics and oxygen availability, which in turn affect the ignition process. [Zhu and Urban \(2024\)](#) further investigated the ignition of oriented strand board (OSB) under varying coverage densities and airflow conditions. Firebrand piles with coverage densities ranging from 0.06 to 0.16 g/cm² were deposited within a 10 × 10 cm area. The findings revealed that ignition probability exhibited a hyperbolic relationship with airflow and coverage density, with smaller firebrands igniting the fuel more rapidly. Increased airflow elevated firebrand surface temperatures, thereby enhancing ignition potential. Moreover, densely accumulated firebrands underwent re-radiation effects, leading to localised temperature increases and faster ignition. Additionally, a correlation between ignition time and firebrand accumulation characteristics based on a theoretical heat transfer analysis was also identified. [Santamaria et al. \(2015\)](#) also conducted bench-scale experiments to investigate smouldering ignition in wooden substrates exposed to firebrand piles with masses and sizes ranging from 0.2 to 98 g/m² and surface areas typically under 100 mm². Results indicated that ignition of wood depended on firebrand size, mass and configuration, with flaming ignition observed at a critical firebrand mass of 60 g.

[Meerpoel-Pietri et al. \(2021\)](#) examined firebrand ignition thresholds by analysing the location, minimum number and mass of firebrands required to ignite different decking slabs. The first decking slab was made of pine, whereas the second was a thermoplastic composed of polypropylene and calcium carbonate. They found that the wooden slab required a minimum mass of 0.31 g of firebrands for ignition, whereas the thermoplastic slab needed at least 0.80 g, indicating that wooden slabs are more susceptible to ignition. Additionally, they observed that ignition occurs when firebrands are deposited in gaps or crevices of the wooden slab and against the legs of the thermoplastic slab, but no ignition occurs when firebrands are deposited on the surface of the slabs.

Influence of structure characteristics

The characteristics of a structural material play a key role in determining its vulnerability to ignition ([Suzuki and Manzello 2020a](#); [Wickramasinghe et al. 2023a](#)). The build-up of firebrands in gaps and openings within the structure, such as the roof, decking and vents, are considered the primary factor contributing to the vulnerability of structures to ignition ([Quarles and Sindelar 2011](#); [Manzello et al. 2020](#); [Nazare et al. 2021](#)) and the initiation of smouldering

([Gellerman and Chien 2023](#); [Wickramasinghe et al. 2023b](#)). For example, studies have examined the ignition behaviour of various wood construction materials. [Kasymov et al. \(2019\)](#) and [Tarakanova et al. \(2020\)](#) examined the ignition behaviour of various wood construction material samples, including plywood, OSB, chipboard, particle board and spruce. Notably, construction materials like plywood and OSB are more resistant to ignition compared with spruce, as they require a larger number of firebrands and have a longer ignition delay time. This was attributed to their composition, which contains synthetic resins. Similarly, [Lauterbach et al. \(2024\)](#) investigated how pressure-treated wood (PTW) and wood-plastic composite (Trex) responded to comparable firebrand conditions. PTW was found to be more susceptible to sustained smouldering across a wide range of airflow settings, whereas Trex showed less susceptibility to pre-leading zone ignition but was more vulnerable to downstream ignition.

Whereas the previous studies focused on wood-based materials, [Wessies et al. \(2019\)](#) examined the vulnerability of various home insulation materials to ignition when exposed to firebrands under varying airflow conditions. The test samples included polyurethane foam, expanded polystyrene (EPS), extruded polystyrene (XPS), flame-retarded and non-flame-retarded denim, and cellulose. Notably, synthetic polymer insulation materials (EPS and XPS) ignite in a flaming mode but do not sustain flaming ignition, as the firebrands melt through the material and then extinguish. In contrast, cellulosic insulation materials are able to sustain flaming ignition as long as there is sufficient airflow. These findings are consistent with those of [Arruda et al. \(2024\)](#), who noted that synthetic materials such as polystyrene foam (XPS also known as Wallmate) and polyvinyl chloride (PVC) materials primarily melt rather than ignite, demonstrating a strong resistance to sustained flaming ignition, with only smouldering being observed. Furthermore, they highlighted that adding thermally resistant paint to woody materials greatly influenced the reduction of flaming ignition behaviour.

In addition to material composition, the shape and configuration of building materials play a key role in determining firebrand ignition susceptibility. [Richter et al. \(2022\)](#) conducted an experimental study to assess the ignition probability of various wooden materials by a pile of smouldering firebrands under wind speeds ranging from 0.5 to 1.4 m/s. In this study, they used five different configurations, namely a flat board and four crevice configurations with different orientations. Notably, the crevice configurations and their orientation had a significant impact on the ignition propensity of the material owing to the enhanced heat flux from the firebrand to the material surface. Additional study by [Manzello et al. \(2009b\)](#) provided valuable insights into the effect of the orientation angles of wooden structures on the ignition likelihood of building materials. In their study, plywood and OSB samples (with dimensions of 206 × 88 mm) were exposed to deposited firebrands at different angles (60°, 90° and 135°) between the two sections of the test sample under airflow

conditions of 1.3 and 2.4 m/s. The results indicated that, at a sample angle of 60°, no ignition was observed for both plywood and OSB at an airflow of 1.3 m/s. However, at the same angle, an increase in airflow to 2.4 m/s resulted in smouldering ignition, which was subsequently followed by flaming ignition.

The key role the configuration of a building plays in the accumulation of firebrands was further explored. [Nguyen and Kaye \(2021\)](#) investigated ember retention on rooftops under varying wind conditions. They noted that internal roof corners and dormers served as areas with high ember retention, increasing the likelihood of ignition in these regions. Additionally, the study demonstrated that, under certain wind conditions, higher roof slopes could unexpectedly lead to increased ember retention. In another study by [Nguyen and Kaye \(2022a\)](#), they quantified firebrand accumulation on building rooftops with various building shapes under wind speed. They experimentally investigated the accumulation of firebrands on rectangular, L-shaped and T-shaped building structures. The results indicated that building shape and wind direction significantly influenced ember accumulation. As noted, the rectangular-shaped building had the lowest accumulation of embers compared with other shapes. Moreover, the orientation of the wind relative to the building significantly influenced ember accumulation. In a subsequent study ([Nguyen and Kaye 2022b](#)), the authors further examined the impact of surrounding buildings on ember accumulation. Their results show that embers tend to accumulate more on rooftops when the target building is surrounded by structures of similar height, with the highest accumulation occurring in closely spaced structures. Similarly, [Quarles and Sindelar \(2011\)](#) highlighted that the wind direction relative to a vent position significantly affects firebrand penetration, with vents positioned perpendicularly to the wind being more susceptible to firebrand entry.

Ignition of structure by firebrand showers

The interaction of firebrand showers with combustible building materials and wood structures is a significant problem in fire science ([Suzuki and Manzello 2020a](#); [Kasymov *et al.* 2023](#)). Firstly, it should be mentioned that this section focuses on studies examining the role of firebrand showers in igniting structural materials, including various firebrand and material types. These studies were not included in the previous sections because they use a different approach. Unlike deposited firebrands, which remain stationary, firebrand showers involve firebrands in motion before they randomly land on the material. This key difference in methodology justifies separating the two sections. Recent developments in firebrand generator technology and associated research have greatly enhanced our understanding of the ignition behaviour of structural materials exposed to firebrand showers ([Manzello *et al.* 2011, 2012](#)). For example, experimental work by [Suzuki *et al.* \(2016\)](#) studied the

vulnerability of wooden assemblies to firebrand showers, both with and without a nearby fuel source. They found that all scenarios were prone to ignition when exposed to firebrand showers and noted that the wooden assemblies themselves produce firebrands. This aligns with findings by [Kasymov *et al.* \(2023\)](#) who investigated the ignition resistance of different wooden structures when exposed to firebrand showers, including a bench element, a compound fence and an inside corner of a building. They noted among the tested structures that a wood fence was the most prone to ignition and required a lower ignition time.

Wind speed plays a crucial role in firebrand accumulation and ignition potential. [Suzuki and Manzello \(2017a, 2021c\)](#) examined the impact of varying wind speeds (4, 6, 8 and 10 m/s) on the accumulation of firebrands in front of two structures separated by different distances. Notably, the most significant accumulation of firebrands occurred at wind speeds of 6 and 8 m/s, generating enough heat to initiate smouldering ignition of the boards covering the floor. However, at wind speeds of 4 and 10 m/s, firebrands were not able to accumulate in a compact zone. Although they found that accumulation in front of structures increased ignition potential, [Manzello and Suzuki \(2019\)](#) suggest that accumulation beneath structures can be even more critical for sustained ignition. Board spacing also significantly influences the potential of ignition. [Manzello and Suzuki \(2019\)](#) demonstrated that wider spacing between deck boards of the sample reduced the required mass of firebrands for sustained smouldering and flaming ignition, as shown in [Fig. 20](#). They explained that multiple firebrands

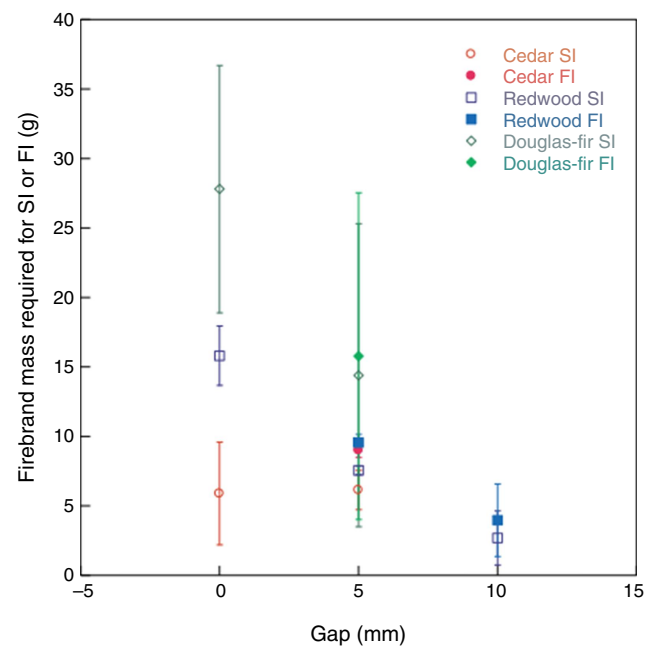


Fig. 20. The relationship between the spacing of decking boards and the required mass of firebrands to sustain ignition ([Manzello and Suzuki 2019](#)) (with permission from Elsevier, licence no. 5820100416315).

fall through these gaps in the boards, resulting in a higher number of firebrands accumulating under the assembly.

Besides wind effects and spacing between boards, the characteristics of the materials themselves also play a crucial role in determining ignition susceptibility. [Manzello and Suzuki \(2014\)](#) investigated the minimum mass of firebrands and the time to flaming ignition of three different types of timber decking made from western red cedar, Douglas-fir and redwood. These decking materials were installed inside a re-entrant corner wall measuring 1.2 m wide and 2.1 m high. The results indicated that the average time to flaming ignition was 437 s for cedar, 934 s for Douglas-fir and 756 s for redwood. Moreover, it was noted that an average firebrand mass of 105 g for cedar, 224 g for Douglas-fir and 182 g for redwood was required to sustain ignition.

In addition to wood structures, roofing assemblies demonstrate different levels of vulnerability to firebrand exposure. [Suzuki and Manzello \(2017b\)](#) and [Suzuki et al. \(2017\)](#) highlighted the vulnerabilities of different tile roofing assemblies, particularly noting that the penetration of firebrands through tile gaps significantly influences ignition susceptibility due to continuous firebrand showers under varying wind speeds. In their experiment, a tile roofing assembly (flat concrete tiles, profiled concrete tiles and flat terracotta tiles) with an angle of 25° was constructed and placed 2 m from the firebrand generator, as shown in [Fig. 21](#). They found that flat tile assemblies had the lowest number of penetrating firebrands compared with another configuration, shown in [Fig. 22](#). Furthermore, wind speed had an effect on the number of firebrands penetrating the roofing assemblies.

The vulnerability of different roofing materials was further explored by [Manzello et al. \(2009a, 2010\)](#), who showed that ceramic tile roofing assemblies were particularly prone to ignition when combined with dried vegetation under the tiles. Moreover, they identified that roof angle plays a

significant role in firebrand vulnerability, with steeper angles (135°) reducing ignition probability owing to decreased firebrand accumulation, whereas moderate angles (60°) led to the highest ignition rates.

Enhancing the resilience of buildings against firebrand attacks

Enhancing the resilience of buildings to withstand firebrand attacks is essential, especially in wildfire-prone areas. This can be achieved by using fire-resistant construction techniques and materials ([Liang et al. 2021](#); [Albert and Liew 2024](#)). Techniques include installing non-combustible roofing, using fire-rated windows and utilising protective vent screens. An effective method involves the application of fine mesh metal screens to vulnerable parts of a building ([Sharifian and Hashempour 2016b](#)). These screens can be installed over vents, eaves and other openings to prevent

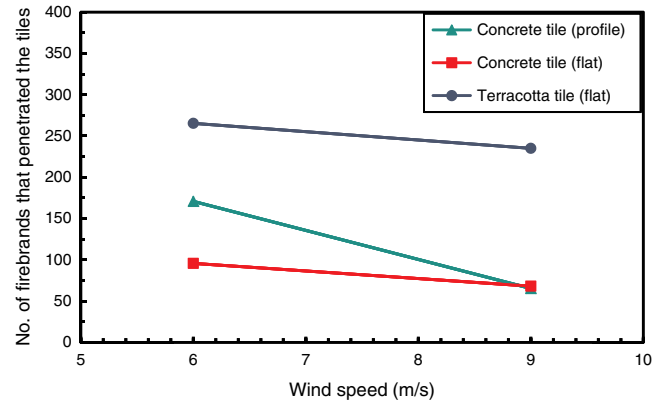


Fig. 22. Number of firebrands that penetrated different types of roof tile under various wind speeds (produced from data in [Suzuki et al. 2017](#)).

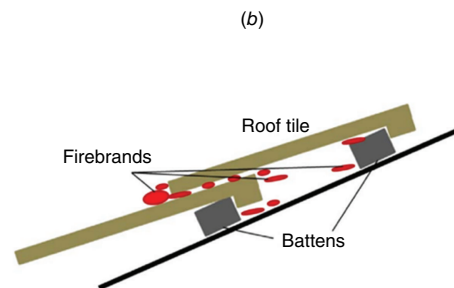
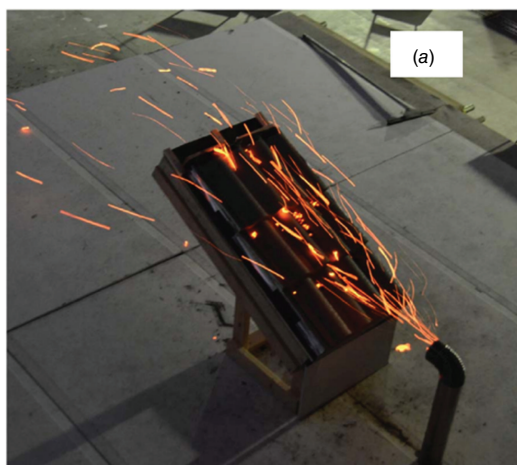


Fig. 21. (a) Roofing assembly exposed to firebrand showers. (b) Schematic of firebrand penetration gaps between the roof tiles ([Suzuki and Manzello 2017b](#)) (with permission from Elsevier, License Number: 5805051333850).

firebrands from entering the building's interior. These screens act as a physical barrier, intercepting embers before they can ignite flammable materials within the structure (Yang and Manzello 2015). For instance, Sharifian Barforoush and du Preez (2022) aimed to quantify the effectiveness of a stainless-steel mesh with an aperture size of 1.67 mm and wire diameter of 0.45 mm at a wind speed of 11.11 m/s against firebrand penetration. The firebrands were generated from red gum and cypress pine vegetation. A plastic sheet holder was attached to the end of the wind tunnel, 2 m downstream of the mesh holder, to capture passing firebrands for later analysis of number and area, thus quantifying the mesh's effectiveness. The experimental results included various interactions between firebrands and the mesh. It was found that ~50–60% of the firebrands passed through the mesh. When the plastic sheet holder was used without the mesh, red gum firebrands caused between 13 and 77 holes, whereas cypress firebrands caused between 85 and 125 holes. However, when the mesh was used, the number of holes significantly decreased to 1–3 for red gum firebrands and to 0–4 for cypress firebrands.

Another experimental study was conducted by Manzello *et al.* (2007b) to assess the effectiveness of steel mesh screens with varying sizes of 1.5, 3 and 6 mm in blocking firebrands from entering a structure through a vent during a firebrand shower. The results revealed that firebrands were able to penetrate all tested screen sizes and result in the ignition of fuel. Sharifian and Hashempour (2016a, 2020) and Hashempour and Sharifian (2017) assessed factors such as screen porosity, screen type (including woven and flat screens), the shape of screen openings (square, circular and rectangular) and the screen's orientation relative to wind direction (perpendicular, leaning forward at 45° and leaning back at 45°) at a wind speed of 14.5 m/s. The study found that both screen porosity and type significantly influenced screen performance, with higher porosity decreasing effectiveness and woven wire screens performing better than flat screens. Larger opening sizes allowed more firebrands to pass through, as shown in Fig. 23a, and the shape of the openings (square, circular, rectangular) showed negligible effect on the penetration ratio. Moreover, the orientation of the screen was crucial, with the perpendicular position being the most effective. Angled screens allowed higher firebrand penetration, as shown in Fig. 23b, which is attributed to a decrease in the effective area of screen openings and a reduction in the perpendicular force of the wind needed to push firebrands through the screen.

Another study conducted by Atwood and Wagenbrenner (2022) explored the efficiency of applying porous fencing, which can act as a windbreak, to alter near-surface flow and effect particle deposition to homes aiming to reduce firebrand attack. They numerically investigated the effectiveness of varying factors including fence height, porosity, wind speed and the size of firebrands on the reduction of firebrand penetration. Results indicated that applying

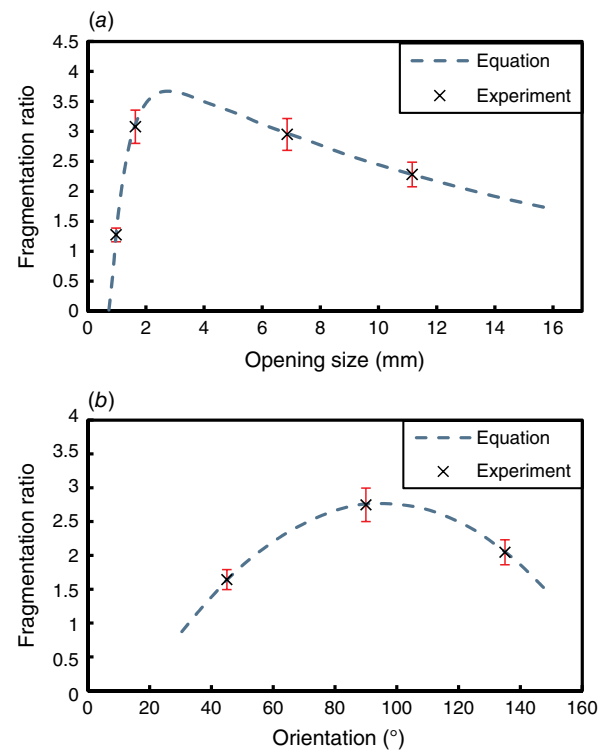


Fig. 23. The effect of (a) opening size, and (b) orientation of a square woven wire screen on the firebrand fragmentation (penetration) ratio (produced from data in Hashempour and Sharifian 2017).

porous fencing around structural material can decrease firebrand penetration by up to 35%.

Knowledge gaps

Several laboratory studies have indicated that the primary factor contributing to the vulnerability of structures is the penetration of firebrands into gaps and crevices. The accumulation of firebrands in these areas can initiate smouldering of combustible materials followed by flaming ignition. Additionally, the configuration of building materials, specifically the spacing and orientation of structural components, significantly influences how these firebrands accumulate and ignite these structures. Despite considerable research on the critical conditions and ignition behaviour of structural materials exposed to firebrands in the WUI, there are still significant gaps in understanding how structural characteristics influence ignition by firebrands, especially in terms of heat transfer mechanisms, which could provide valuable insights for reducing structure losses in wildfires. These studies face considerable challenges in replicating the ignition dynamics of real fires caused by firebrands. Controlled laboratory settings are not able to reproduce the wide variety of firebrand sizes, shapes and thermal properties found in nature, which significantly affect ignition potential. Furthermore, limitations exist in replicating the conditions of real fire such as weather conditions and structure properties. These factors affect

firebrand transport, penetration and accumulation patterns on structural surfaces, which remain an unexplored area of research.

These challenges highlight the need for field studies and advanced modelling techniques to achieve a comprehensive understanding and accurately predict the role of firebrands in structure ignitions. Key knowledge gaps include insufficient data on the impact of firebrand accumulation, their formation into piles, accumulation patterns and their role in the ignition mechanism of the receiving fuel beds. Moreover, there is a lack of data on the combined effects of firebrand showers or firebrand piles with radiation and convection on ignition behaviour. Additional studies are needed to evaluate and explore the ignition resistance of new structural materials and configurations, and assess the effectiveness of adding fire-resistance coating to structural materials and new protective barriers in preventing firebrand penetration. Research should evaluate the effectiveness of these protective materials under various environmental conditions, such as high winds and extended firebrand exposure, to replicate real-world scenarios. To address these gaps, researchers should conduct field studies to observe firebrand behaviour in real wildfires and complement these observations with computational modelling. These models capable of replicating firebrand showers, firebrand accumulation in the form of piles and their interaction with environmental conditions could provide valuable insights into ignition behaviour. Furthermore, laboratory experiments should investigate the effects of structural material properties, firebrand characteristics and environmental conditions on ignition likelihood, enabling a more comprehensive understanding of structure ignitions. These approaches could improve fire risk assessments and inform the development of fire-resistant building materials to reduce the impact of wildfires in the WUI.

Conclusion and recommendations for future work

In order to understand the role of the firebrands in wildfire spotting, this paper provides a comprehensive review of the existing literature on the thermal behaviour of firebrands, focusing on their temperature and heat flux characteristics, as well as the ignition behaviour of natural fuel beds and structures by these firebrands. These small particles or debris, capable of travelling long distances, are considered the primary cause of spotting phenomena and fire spread in WUI areas. This review highlights the significant role of firebrands in igniting fuel beds and structures by thoroughly examining several key factors that influence this process: the impact of firebrand characteristics (e.g. mass, shape and size), the accumulation of firebrands in the form of piles, the properties of fuel beds and structural materials (e.g.

moisture content and type), and environmental conditions (wind speed).

Despite considerable efforts to investigate the thermal behaviour of firebrands and their role in ignition mechanisms, significant knowledge gaps remain. A major area of interest is how the accumulation of firebrands, including mass, porosity, and accumulation area and patterns affects their thermal behaviour (temperature and heat flux). Additionally, there are insufficient data on understanding the ignition thresholds of recipient fuels influenced by firebrands. Therefore, more detailed studies are needed to determine these thresholds for different fuel types, firebrand characteristics, moisture contents and environmental condition that replicate real fire scenarios. Further studies are also needed to understand firebrand ignition under the combined effects of radiant and convective heating. Moreover, there is a crucial need to improve computational and statistical models to more accurately predict the ignition propensity of vegetation and structures by firebrands and to quantify the thermal and burning characteristics of these firebrands. Enhancing these models requires incorporating more detailed physical and chemical processes, improving the representation of firebrand behaviour, refining the understanding of fuel characteristics to better predict ignition likelihood and fire spread. Lastly, researchers should pay attention to the development of fire-resistant building materials capable of withstanding severe heat exposure and preventing firebrand penetration, thereby enhancing the resilience of communities in fire areas.

References

- Abul-Huda YM, Bouvet N (2021) Thermal dynamics of deposited firebrands using phosphor thermometry. *Proceedings of the Combustion Institute* **38**, 4757–4765. doi:10.1016/j.proci.2020.07.098
- Adusumilli S, Blunck D (2022) Energy deposition by firebrands generated from tree-scale burns. In '2022 WSSCI Spring Technical Meeting Organized by the Western States Section of the Combustion Institute, Stanford, CA'.
- Adusumilli S, Blunck DL (2023) Size and energy distribution of firebrands produced from burning trees. *Fire Safety Journal* **138**, 103800. doi:10.1016/j.firesaf.2023.103800
- Alascio JA (2021) Firebrand pile thermal characterization and ignition study of firebrand exposed western red cedar. DRUM – University of Maryland, USA. doi:10.13016/bln8-d4np
- Albert CM, Liew KC (2024) Recent development and challenges in enhancing fire performance on wood and wood-based composites: a 10-year review from 2012 to 2021. *Journal of Bioresources and Bioproducts* **9**, 27–42. doi:10.1016/j.jobab.2023.10.004
- Albini FA (1979) 'Spot fire distance from burning trees: a predictive model.' (Intermountain Forest and Range Experiment Station, USDA Forest Service: US)
- Albini FA (1983) 'Potential spotting distance from wind-driven surface fires.' (USDA Forest Service, Intermountain Forest and Range: US)
- Almeida M, Viegas DX, Miranda AI, Reva V (2011) Effect of particle orientation and of flow velocity on the combustibility of *Pinus pinaster* and *Eucalyptus globulus* firebrand material. *International Journal of Wildland Fire* **20**, 946–962. doi:10.1071/WF09080
- Álvarez C, Moreno G, Valenzuela F, Rivera JI, Ebensperger F, Reszka P, Fuentes A (2023) Use of an electric heater as an idealized firebrand to determine ignition delay time of *Eucalyptus globulus* leaves. *Fire Safety Journal* **141**, 103923. doi:10.1016/j.firesaf.2023.103923

- Arruda MRT, Cantor P, Bicelli A, Branco F (2024) Thermal reaction of firebrand accumulation in construction materials. *Case Studies in Construction Materials* 20, e02985. doi:10.1016/j.cscm.2024.e02985
- Atreya A, Abu-Zaid M (1991) Effect of environmental variables on piloted ignition. *Fire Safety Science* 3, 177–186. doi:10.3801/IAFSS.FSS.3-177
- Atwood L, Wagenbrenner N (2022) A numerical investigation exploring the potential role of porous fencing in reducing firebrand impingement on homes. *Frontiers in Mechanical Engineering* 8, 1059018. doi:10.3389/fmech.2022.1059018
- Baldwin JH, Sunderland PB (2023) Ratio pyrometry of emulated firebrand streaks. *Fire Safety Journal* 136, 103746. doi:10.1016/j.firesaf.2023.103746
- Banagiri S, Meadows J, Lattimer BY (2023) A computational fluid dynamics model to estimate local quantities in firebrand char oxidation. *Journal of Fire Sciences* 41, 241–268. doi:10.1177/07349041231195847
- Bean D, Blunck DL (2021) Sensitivities of porous beds and plates to ignition by firebrands. *Frontiers in Mechanical Engineering* 7, 653810. doi:10.3389/fmech.2021.653810
- Bearinger ED (2021) Factors affecting heat transfer from firebrands and firebrand piles and the ignition of building materials. Available at <https://api.semanticscholar.org/CorpusID:252086242>
- Bearinger E, Lattimer BY, Hodges JL, Rippe C, Kapahi A (2021a) Statistical assessment of parameters affecting firebrand pile heat transfer to surfaces. *Frontiers in Mechanical Engineering* 7, 702181. doi:10.3389/fmech.2021.702181
- Bearinger ED, Hodges JL, Yang F, Rippe CM, Lattimer BY (2021b) Localized heat transfer from firebrands to surfaces. *Fire Safety Journal* 120, 103037. doi:10.1016/j.firesaf.2020.103037
- Bicelli AR, Cantor P, Arruda MR, Tiago C, Bernardes De Assis E, Branco F (2023) Numerical assessment of standard firebrand accumulation curve when transferring temperature to contact surfaces. *Applied Sciences* 13, 9657. doi:10.3390/app13179657
- Burton JE, Filkov AI, Pickering BJ, Penman TD, Cawson JG (2023) Quantifying litter bed ignitability: comparison of a laboratory and field method. *Fire* 6, 24. doi:10.3390/fire6010024
- Campbell-Lochrie Z, Walker-Ravena C, Gallagher M, Skowronski N, Mueller EV, Hadden RM (2021) Investigation of the role of bulk properties and in-bed structure in the flow regime of buoyancy-dominated flame spread in porous fuel beds. *Fire Safety Journal* 120, 103035. doi:10.1016/j.firesaf.2020.103035
- Cantor P, Arruda MRT, Firmo J, Branco F (2023) Development of a standard firebrand accumulation temperature curve for residential wildfire protection system. *Results in Engineering* 17, 100935. doi:10.1016/j.rineng.2023.100935
- Caton SE, Hakes RS, Gorham DJ, Zhou A, Gollner MJ (2017) Review of pathways for building fire spread in the wildland–urban interface. Part I: Exposure conditions. *Fire Technology* 53, 429–473. doi:10.1007/s10694-016-0589-z
- Cawson JG, Pickering BJ, Filkov AI, Burton JE, Kilinc M, Penman TD (2022) Predicting ignitability from firebrands in mature wet eucalypt forests. *Forest Ecology and Management* 519, 120315. doi:10.1016/j.foreco.2022.120315
- Claridge E, Spearpoint M (2013) New Zealand Fire Service response times to structure fires. *Procedia Engineering* 62, 1063–1072. doi:10.1016/j.proeng.2013.08.162
- Cohen JD, Stratton RD (2008) Home destruction examination – Grass Valley fire, Report R5-TP-026b. (USDA Forest Service)
- Cruz MG, Sullivan AL, Gould JS, Sims NC, Bannister AJ, Hollis JJ, Hurley RJ (2012) Anatomy of a catastrophic wildfire: the Black Saturday Kilmore East Fire in Victoria, Australia. *Forest Ecology and Management* 284, 269–285. doi:10.1016/j.foreco.2012.02.035
- De Beer JA, Alascio JA, Stoliarov SI, Gollner MJ (2023a) Analysis of the thermal exposure and ignition propensity of a lignocellulosic building material subjected to a controlled deposition of glowing firebrands. *Fire Safety Journal* 135, 103720. doi:10.1016/j.firesaf.2022.103720
- De Beer JA, Dietz EL, Stoliarov SI, Gollner MJ (2023b) An empirical firebrand pile heat flux model. *Fire Safety Journal* 141, 104004. doi:10.1016/j.firesaf.2023.104004
- Donovan VM, Crandall R, Fill J, Wonkka CL (2023) Increasing large wildfire in the eastern United States. *Geophysical Research Letters* 50, e2023GL107051. doi:10.1029/2023GL107051
- Dossi S, Rein G (2022) Modelling wildfire firebrand accumulation in front of walls perpendicular to the wind. In ‘Advances in Forest Fire Research 2022’ Chapter 2. pp. 706–713. doi:10.14195/978-989-26-2298-9_108
- Dossi S, Wegrzyński W, Rein G (2025) Exploratory Simulations on the effectiveness of sand protection strategies against firebrand accumulation in wildfires. *Fire and Materials* 2025, doi:10.1002/fam.3286
- Dowling VP (1994) Ignition of timber bridges in bushfires. *Fire Safety Journal* 22, 145–168. doi:10.1016/0379-7112(94)90070-1
- Ellis P (2000) The aerodynamic and combustion characteristics of eucalypt bark: a firebrand study. Available at <http://hdl.handle.net/1885/49422>
- Ellis PFM (2011) Fuelbed ignition potential and bark morphology explain the notoriety of the eucalypt messmate ‘stringybark’ for intense spotting. *International Journal of Wildland Fire* 20, 897–907. doi:10.1071/WF10052
- Ellis PFM (2015) The likelihood of ignition of dry-eucalypt forest litter by firebrands. *International Journal of Wildland Fire* 24, 225–235. doi:10.1071/WF14048
- Fang W, Peng Z, Chen H (2021) Ignition of pine needle fuel bed by the coupled effects of a hot metal particle and thermal radiation. *Proceedings of the Combustion Institute* 38, 5101–5108. doi:10.1016/j.proci.2020.05.032
- Fang W, Yang J, Chen H, Zhang L, Guo P, Yuan Y (2023) Effect of wind velocity on smoldering ignition of moist pine needles by a glowing firebrand. *Fire Technology* 60, 501–517. doi:10.1007/s10694-023-01520-6
- Fateev V, Agafontsev M, Volkov S, Filkov A (2017) Determination of smoldering time and thermal characteristics of firebrands under laboratory conditions. *Fire Safety Journal* 91, 791–799. doi:10.1016/j.firesaf.2017.03.080
- Fernandez-Pello AC (2017) Wildland fire spot ignition by sparks and firebrands. *Fire Safety Journal* 91, 2–10. doi:10.1016/j.firesaf.2017.04.040
- Fernandez-Pello AC, Lautenberger C, Rich D, Zak C, Urban J, Hadden R, Scott S, Fereres S (2015) Spot fire ignition of natural fuel beds by hot metal particles, embers, and sparks. *Combustion Science and Technology* 187, 269–295. doi:10.1080/00102202.2014.973953
- Filkov A, Kasymov D, Zima V, Matvienko O (2016) Experimental investigation of surface litter ignition by bark firebrands. *AIP Conference Proceedings* 1698, 060004. doi:10.1063/1.4937859
- Filkov A, Prohanov S, Mueller E, Kasymov D, Martynov P, Houssami ME, Thomas J, Skowronski N, Butler B, Gallagher M, Clark K, Mell W, Kremens R, Hadden RM, Simeoni A (2017) Investigation of firebrand production during prescribed fires conducted in a pine forest. *Proceedings of the Combustion Institute* 36, 3263–3270. doi:10.1016/j.proci.2016.06.125
- Filkov AI, Ngo T, Matthews S, Telfer S, Penman TD (2020) Impact of Australia’s catastrophic 2019/20 bushfire season on communities and environment. Retrospective analysis and current trends. *Journal of Safety Science and Resilience* 1, 44–56. doi:10.1016/j.jnlssr.2020.06.009
- Filkov AI, Tihay-Felicelli V, Masoudvaziri N, Rush D, Valencia A, Wang Y, Blunck DL, Valero MM, Kempna K, Smolka J (2023) A review of thermal exposure and fire spread mechanisms in large outdoor fires and the built environment. *Fire Safety Journal* 140, 103871. doi:10.1016/j.firesaf.2023.103871
- Ganteaume A, Lampin-Maillet C, Guijarro M, Hernando C, Jappiot M, Fontúrbel T, Pérez-Gorostiaga P, Vega JA (2009) Spot fires: fuel bed flammability and capability of firebrands to ignite fuel beds. *International Journal of Wildland Fire* 18, 951–969. doi:10.1071/WF07111
- Ganteaume A, Guijarro M, Jappiot M, Hernando C, Lampin-Maillet C, Pérez-Gorostiaga P, Vega JA (2011) Laboratory characterization of firebrands involved in spot fires. *Annals of Forest Science* 68, 531–541. doi:10.1007/s13595-011-0056-4
- Gaudet B, Simeoni A, Gwynne S, Kuligowski E, Benichou N (2020) A review of post-incident studies for wildland–urban interface fires. *Journal of Safety Science and Resilience* 1, 59–65. doi:10.1016/j.jnlssr.2020.06.010
- Gellerman K, Chien Y-C (2023) Modeling ember behavior and accumulation patterns on and around sample homes during a wildfire. Available at <https://escholarship.org/uc/item/2zz0j0ts>

- Green A, Kaye NB (2019) On the use of sprays to intercept airborne embers during wildfires. *Fire Safety Journal* **108**, 102842. doi:10.1016/j.firesaf.2019.102842
- Hadden RM, Scott S, Lautenberger C, Fernandez-Pello AC (2011) Ignition of combustible fuel beds by hot particles: an experimental and theoretical study. *Fire Technology* **47**, 341–355. doi:10.1007/s10694-010-0181-x
- Hakes RSP, Salehizadeh H, Weston-Dawkes MJ, Gollner MJ (2019) Thermal characterization of firebrand piles. *Fire Safety Journal* **104**, 34–42. doi:10.1016/j.firesaf.2018.10.002
- Hashempour J, Sharifian A (2017) Effective factors on the performance of woven wire screens against leaf firebrand attacks. *Journal of Fire Sciences* **35**, 303–316. doi:10.1177/0734904117709203
- Haynes K, Short K, Xanthopoulos G, Viegas D, Ribeiro LM, Blanchi R (2020) Wildfires and WUI fire fatalities. In 'Encyclopedia of Wildfires and Wildland-Urban Interface (WUI) Fires'. (Ed. SL Manzello) pp. 1–16. (Springer: Cham, Switzerland)
- He Q, Liu N, Xie X, Zhang L, Zhang Y, Yan W (2021) Experimental study on fire spread over discrete fuel bed – Part I: Effects of packing ratio. *Fire Safety Journal* **126**, 103470. doi:10.1016/j.firesaf.2021.103470
- Hedayati F, Bahrani B, Zhou A, Quarles SL, Gorham DJ (2019) A framework to facilitate firebrand characterization. *Frontiers in Mechanical Engineering* **5**, 43. doi:10.3389/fmech.2019.00043
- Henriques-Gomes L (2020) Bushfires death toll rises to 33 after body found in burnt out house near Moruya. The Guardian. Retrieved from <https://www.theguardian.com/australia-news/2020/jan/24/bushfires-death-toll-rises-to-33-after-body-found-in-burnt-out-house-near-moruya>
- Hernández N, Fuentes A, Consalvi JL, Elicer-Cortés JC (2018) Spontaneous ignition of wildland fuel by idealized firebrands. *Experimental Thermal and Fluid Science* **95**, 88–95. doi:10.1016/j.exptthermfluidsci.2018.01.037
- Jervis FX, Rein G (2016a) Experimental study on the burning behaviour of *Pinus halepensis* needles using small-scale fire calorimetry of live, aged and dead samples. *Fire and Materials* **40**, 385–395. doi:10.1002/fam.2293
- Ju X, Lisano M, Hajilou M, Sunderland PB, Stoliarov SI, Yang L, Gollner MJ (2024) Quantification of firebrand generation from WUI fuels for model development: firebrand generation rate, surface temperature and heat release rate. *Proceedings of the Combustion Institute* **40**, 105729. doi:10.1016/j.proci.2024.105729
- Karimpour A, Kaye N (2012) On the stochastic nature of compact debris flight. *Journal of Wind Engineering and Industrial Aerodynamics* **100**, 77–90. doi:10.1016/j.jweia.2011.11.001
- Kasymov D, Filkov A, Baydarov D, Sharypov O (2016) 'Interaction of smoldering branches and pine bark firebrands with fuel bed at different ambient conditions' (SPIE)
- Kasymov D, Agafontsev M, Fateyev VN, Reyno V, Filkov A (2018) 'Critical conditions for the ignition of cedar needle fuel bed as a result of firebrands accumulation. In 'VIII International Conference on Forest Fire Research'. doi:10.14195/978-989-26-16-506_173
- Kasymov DP, Tarakanova VA, Martynov PS, Agafontsev MV (2019) Studying firebrands interaction with flat surface of various wood construction materials in laboratory conditions. *Journal of Physics: Conference Series* **1359**, 012092. doi:10.1088/1742-6596/1359/1/012092
- Kasymov DP, Agafontsev MV, Perminov VV, Loboda EL, Loboda YA, Reino VV, Orlov KE (2023) Ignition resistance of wood building structures exposed to a firebrand shower. *Combustion, Explosion, and Shock Waves* **59**, 206–214. doi:10.1134/S0010508223020119
- Kim DK, Sunderland PB (2019) Fire ember pyrometry using a color camera. *Fire Safety Journal* **106**, 88–93. doi:10.1016/j.firesaf.2019.04.006
- Koo E, Pagni PJ, Weise DR, Woycheese JP (2010) Firebrands and spotting ignition in large-scale fires. *International Journal of Wildland Fire* **19**, 818–843. doi:10.1071/WF07119
- Kramer HA, Mockrin MH, Alexandre PM, Stewart SI, Radloff VC (2018) Where wildfires destroy buildings in the US relative to the wildland-urban interface and national fire outreach programs. *International Journal of Wildland Fire* **27**, 329–341. doi:10.1071/WF17135
- Kwon B, Liao Y-T (2022a) Ignition propensity of structural materials exposed to multiple firebrands in wildland-urban interface (WUI) fires: effects of firebrand distribution and ambient wind. In '2022 Spring Technical Meeting of the Central States Section of the Combustion Institute, Detroit, Michigan'.
- Kwon B, Liao Y-TT (2022b) Effects of spacing on flaming and smoldering firebrands in wildland-urban interface fires. *Journal of Fire Sciences* **40**, 155–174. doi:10.1177/07349041221081998
- Lampin-Maillet C, Mantzavelas A, Galiana L, Jappiot M, Long M, Herrero G, Karlsson O, Iossifina A, Thalia L, Thanassis P (2010). Wildland urban interfaces, fire behaviour and vulnerability: characterization, mapping and assessment. In 'Towards Integrated Fire Management-Outcomes of the European Project Fire Paradox'. (Ed. C Lampin-Maillet) pp. 71–91. (European Forest Institute)
- Lattimer BY, Wong S, Hodges J (2022) A theoretical model to understand some aspects of firebrand pile burning. *Fire Technology* **58**, 3353–3384. doi:10.1007/s10694-022-01303-5
- Lautenberger C, Fernandez-Pello AC (2009) Spotting ignition of fuel beds by firebrands. In 'Computational Methods and Experimental Measurements XIV. Vol. 48' (WIT Transactions on Modelling and Simulation)doi:10.2495/CMEM090541
- Lauterbach A, Lee S, De Beer J, Stoliarov SI, Sunderland PB, Gollner MJ, Filkov AI, Horn GP (2024) Ignition and combustion behavior of pressure treated wood and wood-plastic composite exposed to glowing firebrand piles: impact of air flow velocity, firebrand coverage density and pile orientation. *Fire Safety Journal* **147**, 104198. doi:10.1016/j.firesaf.2024.104198
- Leonard J, Blanchi R (2005) Investigation of bushfire attack mechanisms resulting in house loss in the ACT bushfire 2003. Bushfire CRC Report CMIT Technical Report-2005-478. (Bushfire Co-operative Research Centre: Melbourne)
- Liang C, Du Y, Wang Y, Ma A, Huang S, Ma Z (2021) Intumescent fire-retardant coatings for ancient wooden architectures with ideal electromagnetic interference shielding. *Advanced Composites and Hybrid Materials* **4**, 979–988. doi:10.1007/s42114-021-00274-5
- Lin S, Li C, Conkling M, Huang X, Quarles SL, Gollner MJ (2024a) Smoldering ignition and transition to flaming in wooden mulch beds exposed to firebrands under wind. *Fire Safety Journal* **148**, 104226. doi:10.1016/j.firesaf.2024.104226
- Lin S, Zhang T, Huang X, Gollner MJ (2024b) The initiation of smoldering peat fire by a glowing firebrand. *International Journal of Wildland Fire* **33**, WF23116. doi:10.1071/WF23116
- Lu H, Ip L-T, Mackrory A, Werrett L, Scott J, Tree D, Baxter L (2008) Particle surface temperature measurements with multicolor band pyrometry. *AIChE Journal* **55**, 243–255. doi:10.1002/aic.11677
- Manzello SL (2019) On the importance of firebrand processes in large outdoor fires. *Journal of the Combustion Society of Japan* **61**, 96–100. doi:10.20619/jcombsj.61.196_96
- Manzello S, Suzuki S (2014) Exposing Decking Assemblies to Continuous Wind-Driven Firebrand Showers. In 'Fire Safety Science - Proceedings of the Eleventh International Symposium', Christchurch, NZ. Available at https://tsapps.nist.gov/publication/get_pdf.cfm?pub_id=913383 [accessed 8 May 2025]
- Manzello SL, Suzuki S (2019) Influence of board spacing on mitigating wood decking assembly ignition. *Fire Safety Journal* **110**, 102913. doi:10.1016/j.firesaf.2019.102913
- Manzello SL, Suzuki S (2023) The world is burning: what exactly are firebrands and why should anyone care? *Frontiers in Mechanical Engineering* **8**, doi:10.3389/fmech.2022.1072214
- Manzello SL, Cleary TG, Shields JR, Yang JC (2005a) Urban-wildland fires: on the ignition of surfaces by embers. In 'Proceedings of the 4th Joint Meeting of the US Sections of Combustion Institute'. (Ed. S Turns) pp. 1–8. (Citeseer)
- Manzello S, Shields JR, Cleary TG, Yang JC (2005b). Ignition of mulch by firebrands in Wildland/Urban Interface (WUI) fires. In 'The Joint Meeting of the Sixth Symposium on Fire and Forest Meteorology and the | 19th | Interior West Fire Council Meeting | AMS', 25–27 October 2005, Alberta, 1, CA. pp. 267–270. (International Symposium on Fire and Forest Meteorology)
- Manzello SL, Cleary TG, Shields JR, Yang JC (2006a) Ignition of mulch and grasses by firebrands in wildland-urban interface fires. *International Journal of Wildland Fire* **15**, 427–431. doi:10.1071/WF06031
- Manzello S, Cleary T, Shields J, Yang J (2006b) On the ignition of fuel beds by firebrands. *Fire and Materials* **30**, 77–87. doi:10.1002/fam.901

- Manzello SL, Maranghides A, Mell WE (2007a) Firebrand generation from burning vegetation. *International Journal of Wildland Fire* 16, 458–462. doi:10.1071/WF06079
- Manzello S, Shields J, Yang J, Hayashi Y, Nii D (2007b) On the use of a firebrand generator to investigate the ignition of structures in wildland–urban interface (WUI) fires. In 'International Interflam Conference 11th Proceedings', 3–5 September 2007, London, England. Available at https://tsapps.nist.gov/publication/get_pdf.cfm?pub_id=900080 [accessed 8 May 2025]
- Manzello SL, Cleary TG, Shields JR, Maranghides A, Mell W, Yang JC (2008a) Experimental investigation of firebrands: generation and ignition of fuel beds. *Fire Safety Journal* 43, 226–233. doi:10.1016/j.firesaf.2006.06.010
- Manzello SL, Shields JR, Cleary TG, Maranghides A, Mell WE, Yang JC, Hayashi Y, Nii D, Kurita T (2008b) On the development and characterization of a firebrand generator. *Fire Safety Journal* 43, 258–268. doi:10.1016/j.firesaf.2007.10.001
- Manzello S, Shields J, Hayashi Y, Nii D (2009a) Investigating the vulnerabilities of structures to ignition from a firebrand attack. *Fire Safety Science* 9, 143–154. doi:10.3801/IAFSS.FSS.9-143
- Manzello SL, Park S-H, Cleary TG (2009b) Investigation on the ability of glowing firebrands deposited within crevices to ignite common building materials. *Fire Safety Journal* 44, 894–900. doi:10.1016/j.firesaf.2009.05.001
- Manzello SL, Hayashi Y, Yoneki T, Yamamoto Y (2010) Quantifying the vulnerabilities of ceramic tile roofing assemblies to ignition during a firebrand attack. *Fire Safety Journal* 45, 35–43. doi:10.1016/j.firesaf.2009.09.002
- Manzello SL, Park S-H, Suzuki S, Shields JR, Hayashi Y (2011) Experimental investigation of structure vulnerabilities to firebrand showers. *Fire Safety Journal* 46, 568–578. doi:10.1016/j.firesaf.2011.09.003
- Manzello SL, Suzuki S, Hayashi Y (2012) Exposing siding treatments, walls fitted with eaves, and glazing assemblies to firebrand showers. *Fire Safety Journal* 50, 25–34. doi:10.1016/j.firesaf.2012.01.006
- Manzello SL, Yamada T, Jeffers A, Ohmiya Y, Himoto K, Carlos Fernandez-Pello A (2013) Summary of workshop for fire structure interaction and urban and wildland–urban interface (WUI) fires – Operation Tomodachi fire research. *Fire Safety Journal* 59, 122–131. doi:10.1016/j.firesaf.2013.03.021
- Manzello SL, Suzuki S, Nii D (2017) Full-scale experimental investigation to quantify building component ignition vulnerability from mulch beds attacked by firebrand showers. *Fire Technology* 53, 535–551. doi:10.1007/s10694-015-0537-3
- Manzello SL, Suzuki S, Gollner MJ, Fernandez-Pello AC (2020) Role of firebrand combustion in large outdoor fire spread. *Progress in Energy and Combustion Science* 76, 100801. doi:10.1016/j.peccs.2019.100801
- Maranghides A, Mell W (2011) A case study of a community affected by the Witch and Guejito wildland fires. *Fire Technology* 47, 379–420. doi:10.1007/s10694-010-0164-y
- Matvienko OV, Kasymov DP, Filkov AI, Daneyko OI, Gorbatov DA (2018) Simulation of fuel bed ignition by wildland firebrands. *International Journal of Wildland Fire* 27, 550–561. doi:10.1071/WF17083
- Matvienko O, Kasymov D, Loboda E, Lutsenko A, Daneyko O (2022) Modeling of wood surface ignition by wildland firebrands. *Fire* 5, 38. doi:10.3390/fire5020038
- Matvienko O, Kasymov D, Loboda E, Lutsenko A, Daneyko O (2023) Simulation of the impact of firebrands on the process of the wood layer ignition. *Fire* 6, 148. doi:10.3390/fire6040148
- McGrattan K, Mcdermott R, Weinschenk C, Forney G (2013) 'Fire Dynamics Simulator, Technical Reference Guide', 6th edn. Special Publication (NIST SP). (National Institute of Standards and Technology: Gaithersburg, MD)
- Meerpoel-Pietri K, Tihay-Felicelli V, Santoni P-A (2021) Determination of the critical conditions leading to the ignition of decking slabs by flaming firebrands. *Fire Safety Journal* 120, 103017. doi:10.1016/j.firesaf.2020.103017
- Mensch AE, Wessies SS, Hamins A, Yang JC (2023a) Measuring firebrand heat flux with a thin-skin calorimeter. *Fire Safety Journal* 140, 103859. doi:10.1016/j.firesaf.2023.103859
- Mensch A, Wessies S, Hamins A, Yang J (2023b) Experimental studies on the heat flux of individual firebrands. In '13th US National Combustion Meeting Organized by the Central States Section of the Combustion Institute'. College Station, Texas, USA. https://tsapps.nist.gov/publication/get_pdf.cfm?pub_id=936167 [accessed 8 May 2025]
- Moghtaderi B, Poespowati T, Kennedy EM, Dlugogorski BZ (2007) The role of extinction on the re-ignition potential of wood-based embers in bushfires. *International Journal of Wildland Fire* 16, 547–555. doi:10.1071/WF06029
- Nazare S, Leventon I, Davis R (2021) 'Ignitability of structural wood products exposed to embers during wildland fires: a review of literature. Technical Note (NIST TN)'. (National Institute of Standards and Technology: Gaithersburg, MD)
- Nguyen D, Kaye NB (2021) Experimental investigation of rooftop hot-spots during wildfire ember storms. *Fire Safety Journal* 125, 103445. doi:10.1016/j.firesaf.2021.103445
- Nguyen D, Kaye NB (2022a) Quantification of ember accumulation on the rooftops of isolated buildings in an ember storm. *Fire Safety Journal* 128, 103525. doi:10.1016/j.firesaf.2022.103525
- Nguyen D, Kaye NB (2022b) The role of surrounding buildings on the accumulation of embers on rooftops during an ember storm. *Fire Safety Journal* 131, 103624. doi:10.1016/j.firesaf.2022.103624
- Prohanov S, Filkov A, Kasymov D, Agafontsev M, Reyno V (2020) Determination of firebrand characteristics using thermal videos. *Fire* 3, 68. doi:10.3390/fire3040068
- Qin Y, Zhang Y, Chen Y, Lin S, Huang X (2024) Minimum oxygen supply rate for smouldering propagation: effect of fuel bulk density and particle size. *Combustion and Flame* 261, 113292. doi:10.1016/j.combustflame.2024.113292
- Quarles SL, Sindelar M (2011) Wildfire ignition resistant home design (WIRHD) program: full-scale testing and demonstration final report. (USDA Forest Service Savannah River, New Ellenton, SC: United States)
- Quarles S, Standohar-Alfano C (2018) Ignition potential of decks subjected to an ember exposure. Insurance Institute for Business & Home Safety. Available at <https://ibhs.org/wp-content/uploads/Ignition-Potential-of-Decks-Subjected-to-an-Ember-Exposure.pdf> [verified 7 September 2022]
- Radeloff VC, Helmers DP, Kramer HA, Mockrin MH, Alexandre PM, Bar-Massada A, Butsic V, Hawbaker TJ, Martinuzzi S, Syphard AD, Stewart SI (2018) Rapid growth of the US wildland–urban interface raises wildfire risk. *Proceedings of the National Academy of Sciences* 115, 3314–3319. doi:10.1073/pnas.1718850115
- Ramsey ML, Murphy M, Diaz J (2020) The Camp Fire public report: a summary of the Camp Fire investigation. (Oroville, CA)
- Reszka P, Fuentes A (2014) The Great Valparaiso: fire and fire safety management in Chile. *Fire Technology* 51, 753–758. doi:10.1007/s10694-014-0427-0
- Reszka P, Cruz JJ, Valdivia J, González F, Rivera J, Carvajal C, Fuentes A (2020) Ignition delay times of live and dead *Pinus radiata* needles. *Fire Safety Journal* 112, 102948. doi:10.1016/j.firesaf.2020.102948
- Reveco M, Alvarez C, Gallardo J, Valenzuela F, Severino G, Fuentes A, Reszka P, Demarco R (2024) Effect of moisture content on the spotting ignition of live wildland fuels. *Proceedings of the Combustion Institute* 40, 105275. doi:10.1016/j.proci.2024.105275
- Richter F, Bathras B, Barbetta Duarte J, Gollner MJ (2022) The propensity of wooden crevices to smoldering ignition by firebrands. *Fire Technology* 58, 2167–2188. doi:10.1007/s10694-022-01247-w
- Rissel S, Ridenour K (2013) Ember production during the Bastrop Complex fire. *Fire Management Today* 72, 7–13.
- Rivera J, Hernández N, Consalvi JL, Reszka P, Contreras J, Fuentes A (2020) Ignition of wildland fuels by idealized firebrands. *Fire Safety Journal* 120, 103036. doi:10.1016/j.firesaf.2020.103036
- Salehizadeh H, Hakes RSP, Gollner MJ (2021) Critical ignition conditions of wood by cylindrical firebrands. *Frontiers in Mechanical Engineering* 7, 630324. doi:10.3389/fmech.2021.630324
- Santamaria S, Kempná K, Thomas JC, Houssami ME, Mueller EV, Kasimov D, Filkov AI, Gallagher MR, Skowronski NS, Hadden RM, Simeoni A (2015) Investigation of structural wood ignition by firebrand accumulation. In 'The First International Conference on Structural Safety under Fire & Blast', Glasgow, Scotland, UK.
- Scott S, Hadden R, Yun A, Lautenberger C, Fernandez-Pello AC (2011) Ignition of cellulose fuel beds by hot metal particles. In 'Safety and Security Engineering IV. Vol. 117'. doi:10.2495/SAFE110231

- Sharifian A, Hashempour J (2016a) A novel ember shower simulator for assessing performance of low porosity screens at high wind speeds against firebrand attacks. *Journal of Fire Sciences* **34**, 335–355. doi:10.1177/0734904116655175
- Sharifian A, Hashempour J (2016b) The performance of a woven wire screen against firebrand showers under different wind speeds. In '20th Australasian Fluid Mechanics Conference', Perth, Australia.
- Sharifian A, Hashempour J (2020) Wind tunnel experiments on effects of woven wire screens and buffer zones in mitigating risks associated with firebrand showers. *Australian Journal of Mechanical Engineering* **18**, 156–168. doi:10.1080/14484846.2018.1447225
- Sharifian Barforoush A, du Preez M (2022) Quantifying the effectiveness of a mesh in mitigating burning capabilities of firebrand shower. *Fire* **5**, 150. doi:10.3390/fire5050150
- Song J, Huang X, Liu N, Li H, Zhang L (2017) The wind effect on the transport and burning of firebrands. *Fire Technology* **53**, 1555–1568. doi:10.1007/s10694-017-0647-1
- Sun P, Zhang Y, Sun L, Hu H, Guo F, Wang G, Zhang H (2018) Influence of fuel moisture content, packing ratio and wind velocity on the ignition probability of fuel beds composed of Mongolian oak leaves via cigarette butts. *Forests* **9**, 507. doi:10.3390/f9090507
- Suzuki S, Manzello SL (2017a) Experimental investigation of firebrand accumulation zones in front of obstacles. *Fire Safety Journal* **94**, 1–7. doi:10.1016/j.firesaf.2017.08.007
- Suzuki S, Manzello SL (2017b) Experiments to provide the scientific-basis for laboratory standard test methods for firebrand exposure. *Fire Safety Journal* **91**, 784–790. doi:10.1016/j.firesaf.2017.03.055
- Suzuki S, Manzello SL (2019) Understanding structure ignition vulnerabilities using mock-up sections of attached wood fencing assemblies. *Fire and Materials* **43**, 675–684. doi:10.1002/fam.2716
- Suzuki S, Manzello SL (2020a) Experimental study on vulnerabilities of Japanese-style tile roof assemblies to firebrand exposures. *Fire Technology* **56**, 2315–2330. doi:10.1007/s10694-020-00982-2
- Suzuki S, Manzello SL (2020b) Role of accumulation for ignition of fuel beds by firebrands. *Applications in Energy and Combustion Science* **1–4**, 100002. doi:10.1016/j.jaecs.2020.100002
- Suzuki S, Manzello SL (2021a) Ignition vulnerabilities of combustibles around houses to firebrand showers: further comparison of experiments. *Sustainability* **13**, 2136. doi:10.3390/su13042136
- Suzuki S, Manzello SL (2021b) Investigating coupled effect of radiative heat flux and firebrand showers on ignition of fuel beds. *Fire Technology* **57**, 683–697. doi:10.1007/s10694-020-01018-5
- Suzuki S, Manzello SL (2021c) Investigating the effect of structure to structure separation distance on firebrand accumulation. *Frontiers in Mechanical Engineering* **6**, 628510. doi:10.3389/fmech.2020.628510
- Suzuki S, Manzello SL (2021d) Toward understanding ignition vulnerabilities to firebrand showers using reduced-scale experiments. *Fire and Materials* **46**, 809–817. doi:10.1002/fam.3027
- Suzuki S, Manzello SL (2023) Experimental and theoretical approaches to elucidate fuel bed ignition exposed to firebrand showers and radiant heat. *International Journal of Heat and Mass Transfer* **202**, 123740. doi:10.1016/j.ijheatmasstransfer.2022.123740
- Suzuki S, Manzello SL, Kagiya K, Suzuki J, Hayashi Y (2014) Ignition of mulch beds exposed to continuous wind-driven firebrand showers. *Fire Technology* **51**, 905–922. doi:10.1007/s10694-014-0425-2
- Suzuki S, Johnsson E, Maranghides A, Manzello SL (2016) Ignition of wood fencing assemblies exposed to continuous wind-driven firebrand showers. *Fire Technology* **52**, 1051–1067. doi:10.1007/s10694-015-0520-z
- Suzuki S, Nii D, Manzello SL (2017) The performance of wood and tile roofing assemblies exposed to continuous firebrand assault. *Fire and Materials* **41**, 84–96. doi:10.1002/fam.2372
- Tao Z, Bathras B, Kwon B, Biallas B, Gollner MJ, Yang R (2021) Effect of firebrand size and geometry on heating from a smoldering pile under wind. *Fire Safety Journal* **120**, 103031. doi:10.1016/j.firesaf.2020.103031
- Tarakanova VA, Kasymov DP, Galtseva OV, Chicherina NV (2020) Experimental characterization of firebrand ignition of some wood building materials. *Bulletin of the Karaganda University 'Physics Series'* **100**, 14–21. doi:10.31489/2020ph4/14-21
- Tarifa CS, Del Notario P, Moreno FG (1965) On the flight paths and lifetimes of burning particles of wood. *Symposium (International) on Combustion* **10**, 1021–1037.
- Thomas D, Butry D, Gilbert S, Webb D, Fung J (2017) The costs and losses of wildfires. *NIST Special Publication* **1215**, 1–72.
- Thomas JC, Mueller EV, Hadden RM (2018) Chapter 4 - Fire at the Wildland Urban Interface. In 'Estimating net heat flux from surrogate firebrand accumulations using an inverse heat transfer approach'. (Ed. DX Viegas) *Advances in Forest Fire Research*. pp. 769–779. (University of Coimbra: Portugal)
- Thomas JC, Mueller EV, Gallagher MR, Clark KL, Skowronski N, Simeoni A, Hadden RM (2021) Coupled assessment of fire behavior and firebrand dynamics. *Frontiers in Mechanical Engineering* **7**, 650580. doi:10.3389/fmech.2021.650580
- Tiernan F, O'Mallon E (2020) Australia's 2019–20 bushfire season. *The Canberra Times*, 10 January 2020.
- Ulpiani G, Ranzi G, Santamouris M (2020) Experimental evidence of the multiple microclimatic impacts of bushfires in affected urban areas: the case of Sydney during the 2019/2020 Australian season. *Environmental Research Communications* **2**, 065005. doi:10.1088/2515-7620/ab9e1a
- Urban JL, Zak CD, Fernandez-Pello C (2015) Cellulose spot fire ignition by hot metal particles. *Proceedings of the Combustion Institute* **35**, 2707–2714. doi:10.1016/j.proci.2014.05.081
- Urban JL, Zak CD, Song J, Fernandez-Pello C (2017) Smoldering spot ignition of natural fuels by a hot metal particle. *Proceedings of the Combustion Institute* **36**, 3211–3218. doi:10.1016/j.proci.2016.09.014
- Urban JL, Zak CD, Fernandez-Pello C (2018) Spot fire ignition of natural fuels by hot aluminum particles. *Fire Technology* **54**, 797–808. doi:10.1007/s10694-018-0712-4
- Urban JL, Song J, Santamaria S, Fernandez-Pello C (2019a) Ignition of a spot smolder in a moist fuel bed by a firebrand. *Fire Safety Journal* **108**, 102833. doi:10.1016/j.firesaf.2019.102833
- Urban JL, Vicariotto M, Dunn-Rankin D, Fernandez-Pello AC (2019b) Temperature measurement of glowing embers with color pyrometry. *Fire Technology* **55**, 1013–1026. doi:10.1007/s10694-018-0810-3
- Urban J, Parker WJ, Luebbers GE (2004) Surface temperature measurements on burning materials using an infrared pyrometer: accounting for emissivity and reflection of external radiation. *Fire and Materials* **28**, 33–53. doi:10.1002/fam.844
- Valenzuela F, Rivera J, Ebersperger F, Alvarez C, Reszka P, Auat Cheein F, Fuentes A (2023) Ignition of wildland fuels exposed to a time-decreasing incident heat flux. *Combustion Science and Technology* **195**, 3596–3611. doi:10.1080/00102202.2023.2241201
- Viegas DX (2018) Wildfires in Portugal. *Fire Research* **2**, 52. doi:10.4081/fire.2018.52
- Viegas DX, Almeida M, Raposo J, Oliveira R, Viegas CX (2014) Ignition of Mediterranean fuel beds by several types of firebrands. *Fire Technology* **50**, 61–77. doi:10.1007/s10694-012-0267-8
- Wadhvani R, Sullivan C, Wickramasinghe A, Kyng M, Khan N, Moinuddin K (2022) A review of firebrand studies on generation and transport. *Fire Safety Journal* **134**, 103674. doi:10.1016/j.firesaf.2022.103674
- Wang K, Wang S, Huang X (2025) Hot-particle ignition of typical fuels in the Wildland-Urban Interface and subsequent fire behaviors. *Fire and Materials* **2025**. doi:10.1002/fam.3276
- Wang S, Huang X, Chen H, Liu N (2017) Interaction between flaming and smoldering in hot-particle ignition of forest fuels and effects of moisture and wind. *International Journal of Wildland Fire* **26**, 71–81. doi:10.1071/WF16096
- Wang S, Thomsen M, Huang X, Fernandez-Pello C (2024) Spot ignition of a wildland fire and its transition to propagation. *International Journal of Wildland Fire* **33**, WF23207. doi:10.1071/WF23207
- Warey A (2018) Influence of thermal contact on heat transfer from glowing firebrands. *Case Studies in Thermal Engineering* **12**, 301–311. doi:10.1016/j.csite.2018.04.018
- Wessies SS, Ezekoye OA (2022a) Cooling of heated solid cylinder supported on bedded and embedded substrates by impinging air jet. *Journal of Thermal Science and Engineering Applications* **14**, 011009. doi:10.1115/1.4050837
- Wessies SS, Ezekoye OA (2022b) A framework for determining the ignition signatures in a fuel bed due to firebrand deposition. *Fire Technology* **58**, 3439–3461. doi:10.1007/s10694-022-01316-0
- Wessies SS, Yang JC (2023) Convective heat transfer correlation for a single surrogate firebrand and a simplified firebrand pile on a flat

- plate using naphthalene sublimation in heated air flow. *Fire Safety Journal* **140**, 103858. doi:10.1016/j.firesaf.2023.103858
- Wessies SS, Chang MK, Marr KC, Ezekoye OA (2019) Experimental and analytical characterization of firebrand ignition of home insulation materials. *Fire Technology* **55**, 1027–1056. doi:10.1007/s10694-019-00818-8
- Wickramasinghe A, Khan N, Filkov AI, Moinuddin KAM (2023a) Physics-based modelling for mapping firebrand flux and heat load on structures in the wildland–urban interface. *International Journal of Wildland Fire* **32**, 1576–1599. doi:10.1071/WF22119
- Wickramasinghe A, Khan N, Filkov A, Moinuddin K (2023b) Quantifying firebrand and radiative heat flux risk on structures in mallee/mulga-dominated wildland–urban interface: a physics-based approach. *Fire* **6**, 466. doi:10.3390/fire6120466
- Wong S, Hodges JL, Lattimer BY (2022) Impact of ash layer retention on heat transfer in piles of vegetation and structure firebrands. *Fire Safety Journal* **134**, 103694. doi:10.1016/j.firesaf.2022.103694
- Yan W, Liu N, Zhu H, Chen H, Xie X, Gao W, Du Z (2024) Firebrand burning under wind: an experimental study. *International Journal of Wildland Fire* **33**, WF23151. doi:10.1071/WF23151
- Yang G, Ning J, Shu L, Zhang J, Yu H, Di X (2022) Spotting ignition of larch (*Larix gmelinii*) fuel bed by different firebrands. *Journal of Forestry Research* **33**, 171–181. doi:10.1007/s11676-020-01282-9
- Yang J, Peng X, Urban J, Huang W, Wang H, Wang S, Hu Y (2024) Computational study on the glowing combustion of a wooden ember landing on a non-reacting substrate. *Journal of Fire Sciences* **43**, 33–57. doi:10.1177/07349041241256986
- Yang JC, Manzello SL (2015) A dimensional analysis on firebrand penetration through a mesh screen. *Fuel* **160**, 114–116. doi:10.1016/j.fuel.2015.07.098
- Yin P, Liu N, Chen H, Lozano JS, Shan Y (2014) New correlation between ignition time and moisture content for pine needles attacked by firebrands. *Fire Technology* **50**, 79–91. doi:10.1007/s10694-012-0272-y
- Zak CD, Murphy DC, Fernandez-Pello AC (2013) ‘Understanding ignition of natural fuels by heated particles.’ (Safety and Security Engineering V)
- Zak CD, Urban JL, Fernandez-Pello C (2014) Characterizing the flaming ignition of cellulose fuel beds by hot steel spheres. *Combustion Science and Technology* **186**, 1618–1631. doi:10.1080/00102202.2014.935612
- Zhou A, Quarles S, Weise D (2019) Final report: fire ember production from wildland and structural fuels. JFSP Project ID, 15-1. No. 15-1-04-4. (North Carolina State University: Raleigh, NC, USA)
- Zhu L, Urban JL (2023) Cooperative spot ignition by idealized firebrands: impact of thermal interaction in the fuel. *Fire Safety Journal* **135**, 103701. doi:10.1016/j.firesaf.2022.103701
- Zhu L, Urban JL (2024) Analyzing the ignition capabilities of glowing firebrand accumulations. *Proceedings of the Combustion Institute* **40**, 105746. doi:10.1016/j.proci.2024.105746

Data availability. Data sharing is not applicable as no new data were generated or analysed during this study.

Conflicts of interest. The authors declare they have no conflicts of interest.

Declaration of funding. This research did not receive any specific funding.

Acknowledgements. We wish to thank Dr Eric V. Mueller, Fire Research Division, National Institute of Standards and Technology for his valuable insights throughout this work. Alex Filkov was funded by the ARC Discovery ‘Understanding the Origin and Development of Extreme and Mega Bushfires: Merging Fire Fronts’ project.

Author affiliations

^ASchool of Engineering and Technology, University of New South Wales (UNSW), Canberra, ACT 2600, Australia.

^BFaculty of Science, University of Melbourne, 4 Water Street, Creswick, 3350, Australia.